Multitarget Multisensor Tracking in the Presence of Wakes

ANDERS RØDNINGSBY
YAAKOV BAR-SHALOM
ODDVAR HALLINGSTAD
JOHN GLATTETRE

In this paper we focus on targets which, in addition to reflecting signals themselves, also have a trailing path behind them, called a wake, which causes additional detections. When the detections are fed to a tracking system like the probabilistic data association filter (PDAF), the estimated track can be misled and sometimes lose the real target because of the wake. This problem becomes even more severe in multitarget environments where targets are operating close to each other in the presence of wakes. To prevent this, we have developed a probabilistic model of the wakes in a multitarget environment. This model is used to augment the joint probabilistic data association filter (JPDAF) for both coupled and decoupled filtering.

This paper provides a systematic comparison of the standard data association filters (PDAF and JPDAF) and their modified versions presented here in a multitarget multisensor environment. Simulations of two targets with wakes in four different scenarios show that this modification gives good results and the probability of lost tracks is significantly reduced. The targets are observed by two sensors and it is shown that tracks estimated in a centralized fusion configuration are better than those from the local sensors. It is also shown that applying the wake model to targets that do not generate a wake, yields almost no deterioration of the tracking performance.

Manuscript received October 8, 2008; revised February 16, 2009; released for publication June 24, 2009.

Refereeing of this contribution was handled by Dr. Yvo Boers.

Authors' addresses: A. Rødningsby and O. Hallingstad, University Graduate Center, NO-2027 Kjeller, Norway; Y. Bar-Shalom, University of Connecticut, U-2157 Storrs, CT; J. Glattetre, Kongsberg Maritime, NO-3191 Horten, Norway.

1. INTRODUCTION

Targets in real tracking scenarios may be detected by their reflection of signals emitted from a radar [6], a sonar [26], or by the use of optical sensors [24]. In addition to target-originated measurements there will also be a number of detections due to noise and clutter, called false alarms. A well-known tracking method to handle targets in clutter is the probabilistic data association filter (PDAF) [3, ch. 3.4]. The PDAF accounts for the measurement origin uncertainty by calculating for each validated measurement at the current time the association probabilities to the target of interest.

In a multitarget environment [5] the association of measurements is more problematic because the individual targets no longer can be considered separately as in the PDAF. For this purpose the joint probabilistic data association filter (JPDAF) [3, ch. 6.2], [14] was developed to consider a known number of targets in the data association simultaneously. This method evaluates the measurement-to-target association probabilities for the latest set of measurements and then combines them into the state estimates. In the JPDAF the targets' states, conditioned on the past, are assumed independently distributed so that filtering can be done decoupled. As an alternative, the targets' states, given the past, can be considered as correlated. This leads to the joint probabilistic data association coupled filter (JPDACF) [2], [3, pp. 328–329], where the correlation between the targets' estimation errors is accounted for. A modified version of the JPDACF, called coupled data association filter (CPDA), was presented in [9] to also account for partial target detections. In this paper an equivalent filter to the CPDA, but where the covariance calculation is in symmetrical form (to avoid numerical problems experienced by the CPDA), is modified to also account for targets in the presence of wakes. This filter is called modified JPDACF.

A more powerful source of false measurements than those due to noise and clutter, is the wake phenomenon that appears behind certain targets. This could be air bubbles from a diver, the wake behind a ship, or the wake from ballistic vehicles in the re-entry stage. One possible approach to this problem is to handle both the target and the wake behind it as an extended target. A problem with this approach is the varying and unknown size of the wake which may reach far behind the target yielding a large bias. In this paper the wake is not considered as part of the target, but rather as a special kind of clutter. When these measurements are fed to the tracking system, it becomes important to associate them correctly to prevent a lost track. In [1] a probabilistic editing method is used to handle the wake-dominated measurements in the tracking algorithm. This probabilistic editing method is based on a single measurement extracted for each time step, and that this measurement originates from either the tar-

get or the wake. In [21] a modified PDAF is developed to handle false measurements originating from the bubbles behind a diver (the wake). This modified single target tracking method does not restrict the number of false measurements for each time step, but assumes a set of measurements where each false measurement originates from either random clutter or the wake. In this paper we extend the modified PDAF to handle multiple targets in the presence of wakes. A probabilistic wake model is used for each target in the multitarget environment that has a wake behind it. These single wake models are combined to form a joint wake model, and the modified JPDAF and JPDACF are developed to incorporate this additional joint wake model.

In recent years there has been an extensive interest in using multiple sensors in surveillance systems. This leads to data fusion where there exist several possible configurations [3, ch. 8.2]. Primarily due to the bandwidth constraints in real systems, it is sometimes not feasible to transmit all measurement information to a fusion center (centralized configuration). Instead, only local estimates are transmitted to a fusion center (at a reduced rate), and a track-to-track association followed by track fusion is carried out (decentralized configuration). However, the best performance is achieved using the centralized configurations where all measurements are transmitted from the local sensors to a fusion center. In this paper we use the centralized configuration with sequential filtering [3, p. 88] where the global estimate is updated by the measurements from each local sensor, one sensor at the time.

In Section 2 the tracking problem in the presence of a wake is reviewed for a single target. In Section 3 the modified JPDAF is developed for a multitarget environment, and the modified version of the JPDACF, which accounts for partial target detections, is derived. In Section 4 a brief review of multisensor tracking is given. The data association methods are then compared in Section 5 by simulations of two targets with wakes in four different multisensor scenarios, before conclusions are given in Section 6.

2. BACKGROUND

2.1. Model of Tracking

The standard discrete linear model in tracking is

$$x_{k+1} = Fx_k + v_k, \qquad z_k = Hx_k + w_k \tag{1}$$

where

x :	target state	F :	transition matrix
z :	measurement	H :	measurement matrix
v :	process noise	w :	measurement noise
k :	time index		

The process and measurement noises are assumed independent, white and Gaussian with covariance matrices

$$E\{v_k v_k^T\} = Q \qquad \text{and} \qquad E\{w_k w_k^T\} = R. \tag{2}$$

For this system, a Kalman filter is optimal as long as the measurement z_k originates from the target at each time k. In many real world problems this is unfortunately not true due to the presence of false measurements originating from noise and clutter. Instead, a set of m_k measurements $Z_k = \{z_k(1), z_k(2), \ldots, z_k(m_k)\}$ is available at time k so that data association is needed. A simple and efficient method to solve this problem is the PDAF.

2.2. Standard PDAF

The approach of the PDAF is to calculate the association probabilities for each validated measurement (that falls in a gate around the predicted measurement) at the current time to the target of interest. The posterior track probability density is therefore a mixture of Gaussian probability density functions (pdf), but is then forced back to Gaussianity by moment-matching for the succeeding scan. For a derivation of the PDAF see [3, ch. 3.4], and in the following a brief overview of the PDAF will be given.

Assume that the target state at time $k-1$ is estimated as $\hat{x}_{k-1|k-1}$ with associated covariance $P_{k-1|k-1}$. This means that the estimate is conditioned on the entire past up to time $k-1$. Then the following assumptions are made:

a) The track is already initialized.

b) The past information about the target is summarized approximately by the Gaussian pdf

$$p(x_k \mid Z^{k-1}) \approx \mathcal{N}(x_k; \hat{x}_{k|k-1}, P_{k|k-1}) \tag{3}$$

where

$$Z^{k-1} = \{Z_0, Z_1, \ldots Z_{k-1}\}. \tag{4}$$

c) A validation region or gate is set up for each time step to select the candidate measurements for association.

d) At time k there are m_k validated measurements but at most one of them can be target-originated. The rest are assumed to be due to i.i.d. uniformly spatially distributed false alarms, independently across time.

e) Detections of the real target occur independently over time with known detection probability P_{D}.

At each time k, the algorithm goes through the following steps:

1) Predict the target state, associated covariance and measurement at time k based on the estimates at $k-1$:

$$\begin{aligned} \hat{x}_{k|k-1} &= F\hat{x}_{k-1|k-1} \\ P_{k|k-1} &= FP_{k-1|k-1}F^T + Q \\ \hat{z}_{k|k-1} &= H\hat{x}_{k|k-1}. \end{aligned} \tag{5}$$

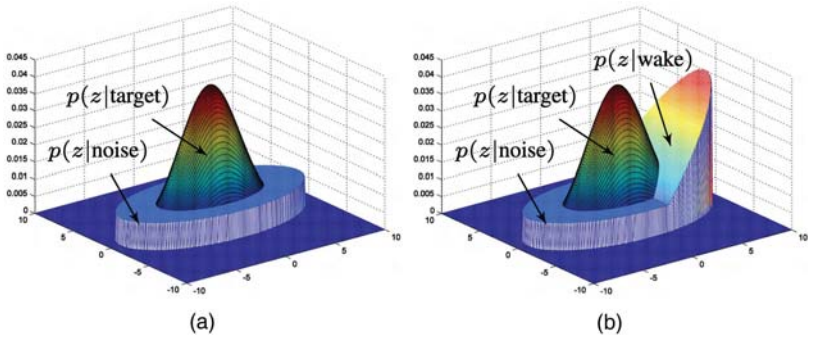

Fig. 1. Illustration of the pdfs for the measurements originating from the target, noise or wake in: (a) regular PDAF, (b) modified PDAF with wake model.

2) Compute the innovation covariance for the true (target-originated) measurement

$$S_k = HP_{k|k-1}H^T + R \tag{6}$$

and use S_k to form the measurement validation gate where the validated measurements Z_k result in m_k innovations:

$$\nu_k(i) = z_k(i) - \hat{z}_{k|k-1} \qquad i = 1,\ldots,m_k, \tag{7}$$

3) Calculate the association probabilities $\beta_k(i)$, $i = 1,\ldots,m_k$ that measurement $z_k(i)$ originates from the true target, and $\beta_k(0)$ as the probability that all measurements are false alarms

$$\beta_k(i) = \begin{cases} ce^{-(1/2)\nu_k(i)^T S_k^{-1}\nu_k(i)} & i = 1,\ldots,m_k \\ c|2\pi S_k|^{1/2} m_k \dfrac{1 - P_G P_D}{V_k P_D} & i = 0 \end{cases}. \tag{8}$$

Here c is a normalizing constant to ensure that $\sum_{i=0}^{m_k}\beta_k(i) = 1$, V_k is the volume of the gate and P_G is the probability that the true measurement falls inside the gate. In (8) a diffuse prior [3, p.135] is used for the point mass function (pmf) of the number of false measurements in the validation region.

4) Calculate the Kalman gain and the combined innovation

$$W_k = P_{k|k-1}H^T S_k^{-1} \qquad \text{and} \qquad \nu_k = \sum_{i=1}^{m_k}\beta_k(i)\nu_k(i) \tag{9}$$

to update the track according to

$$\hat{x}_{k|k} = \hat{x}_{k|k-1} + W_k\nu_k. \tag{10}$$

5) The state estimation covariance is updated by

$$\begin{aligned} P_{k|k} = {} & \beta_k(0)P_{k|k-1} \\ & + [1 - \beta_k(0)](P_{k|k-1} - W_k S_k W_k^T) \\ & + W_k\left[\sum_{i=0}^{m_k}\beta_k(i)\nu_k(i)\nu_k(i)^T - \nu_k\nu_k^T\right]W_k^T \end{aligned} \tag{11}$$

where the last term in (11) is the "spread of the innovations."

2.3. Modified PDAF

Targets with a wake behind them may cause detections from the wake that mislead the tracking algorithm and are likely to result in a lost track. This is because the uniform distribution assumption for the false measurements (assumption (d) in Section 2.2) is violated. To prevent this, an extension of the regular PDAF incorporating a special probabilistic model of the wake was developed in [21]. The PDAF with the wake model is illustrated in Fig. 1. The modified PDAF takes into account that the false measurements can originate from either the wake with pdf $p_W(\cdot)$ with a priori probability P_W, or from i.i.d. uniformly distributed noise/clutter with a priori probability $1 - P_W$, independently across time. This modification affects the PDA in the calculation of the $\beta_k(i)$ in (8) and yields

$$\beta_k(i) = \begin{cases} c\dfrac{e^{-(1/2)\nu_k(i)^T S_k^{-1}\nu_k(i)}}{V_k\left[\dfrac{1-P_W}{V_k} + \dfrac{P_W}{P_{GW}}p_W(z_k(i))\right]} & i = 1,\ldots,m_k \\ c|2\pi S_k|^{1/2} m_k \dfrac{1 - P_G P_D}{V_k P_D} & i = 0 \end{cases}. \tag{12}$$

The bracketed parenthesis in the denominator in $\beta_k(i)$ for $i = 1,\ldots,m_k$ is the pdf of a false measurement

$$\begin{aligned} & p(z_k(i) \mid \text{measurement } i \text{ is false}) \\ & \quad = \frac{1 - P_W}{V_k} + \frac{P_W}{P_{GW}}p_W(z_k(i)) \end{aligned} \tag{13}$$

where P_{GW} is used to account for restricting the density of the wake model $p_W(z_k(i))$ to the validation gate. The calculation of P_{GW} for a linear $p_W(\cdot)$ is presented in detail in [21]. As expected, in the limit as P_W goes to zero, (12) becomes (8).

2.4. Track Formation and Termination

The data association filters discussed above assume that the track is already initialized, and when a track

is established, there are no included rules for how to terminate the track. Hence, procedures for formation and termination of tracks are necessary. A simple and common method to initialize tracks is the two-point differencing method [4, p. 247]. Any successive pair of detections within a maximum distance based on target maximum motion parameters and measurement noise variances initiates a preliminary track. This preliminary track, containing the initial state and the corresponding covariance, can now initialize the PDAF. To reduce the amount of false tracks, a "p/q" logic-based track formation procedure can be used. In this procedure a preliminary track has to receive measurements for a minimum of p time steps during the first q scans to become valid.

To terminate a track a logic suitable for the application is needed, and a set of rules has to be made. The rules used in this paper, called termination events, are described in Section 5.4. It should also be noted that in some filters, such as the integrated probabilistic data association filter (IPDAF) [18] or the version of the interacting multiple model probabilistic data association filter (IMMPDAF) presented in [3, ch. 4.4], the track formation and termination are included.

3. PROBABILISTIC DATA ASSOCIATION FOR MULTIPLE TARGETS IN THE PRESENCE OF WAKES

In a multitarget environment the data association algorithm needs to handle situations where a measurement could originate from different targets. For this purpose, the JPDAF was developed, and a derivation of this standard algorithm is given in [3, ch. 6.2]. Another problem arises when these targets have wakes behind them that result in misleading wake detections. In this section we will modify the JPDAF to handle this problem.

3.1. Assumptions

Assume there is a known number N_T of established targets at time $k-1$. Notice that these targets are already initialized, e.g., by the method in Section 2.2. For each target t, where $t = 1,\ldots,N_T$, the target state is estimated as $\hat{x}^t_{k-1|k-1}$ with associated covariance $P^t_{k-1|k-1}$. Then the following assumptions are made:

a) Measurements from one target can fall in the validation gate of a neighboring target.

b) The past information about target t is summarized approximately by the Gaussian pdf

$$p(x^t_k \mid Z^{k-1}) \approx \mathcal{N}(x^t_k; \hat{x}^t_{k|k-1}, P^t_{k|k-1}). \tag{14}$$

c) At time k there are m_k validated measurements in the union of their validation gates, but for each target t at most one measurement can be target-originated. The rest are assumed to be due to the wakes with pdf $p_W(\cdot)$ with a priori probability P_W, or from i.i.d. uniformly distributed noise/clutter with a priori probability $1-P_W$, independently across time.

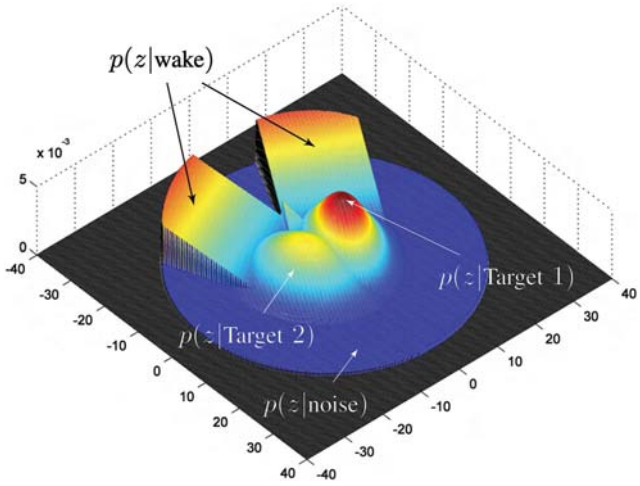

Fig. 2. Probability density functions for two targets with crossing trajectories. The distributions of the targets are Gaussian and overlap each other. Each wake behind the two targets is modeled as a pdf, linearly increasing from the target and backwards, and the sum of each single target's wake model forms the joint wake model. The noise/clutter is uniformly spatially distributed inside the joint validation region.

In Fig. 2 an example of the pdfs for two targets that are starting to cross each other is shown. Here both targets have a wake behind them, and the joint wake model (the sum of each target's single wake model) increases linearly behind the targets inside the joint validation region. The joint validation region contains all the candidate measurements, and restricts the spatially uniform distribution representing the noise/clutter. It should be noted that the linearly increasing wake models are not developed to approach the true density of the wake since the wake density would seemingly be higher close to the targets rather than farther away. Such an approach would easily misassociate true target-originated measurements as wake-originated ones. At the same time, in practice, a false wake-originated measurement is less detrimental when it is very close to the true target than farther behind. The adopted wake model is therefore a pragmatic approach to let the probability of having a wake-originated measurement instead of a target-originated one increase with the distance behind the true target. Further details about the joint wake model and the validation region are given in Appendix A.

3.2. Joint Association Events

Define the validation matrix Ω to represent all feasible association events at time k (the time index k is omitted for simplicity where it does not cause confusion)

$$\Omega = [\omega(j,t)] \qquad j = 1,\ldots,m \quad \text{and} \quad t = 0,\ldots,N_T. \tag{15}$$

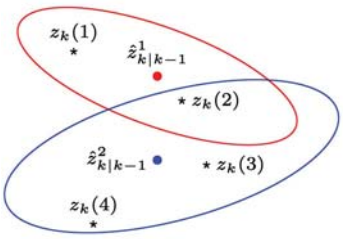

$$\Omega = \begin{array}{c|ccc} j\backslash t & 0 & 1 & 2 \\ \hline 1 & 1 & 1 & 0 \\ 2 & 1 & 1 & 1 \\ 3 & 1 & 0 & 1 \\ 4 & 1 & 0 & 1 \end{array}$$

Fig. 3. Two targets with a measurement in the intersection of their validation gates are shown with corresponding validation matrix Ω.

Here, $\omega(j,t)$ is a binary element indicating whether measurement j lies in the validation gate of target t. The index $t = 0$ means that the measurement is from none of the targets and therefore it is a false measurement. An example where a measurement may originate from either of two targets, i.e., it lies in both targets' validation gates, is shown with the corresponding validation matrix Ω in Fig. 3. For all these possible joint association events, conditional probabilities have to be derived.

A joint association event Θ describes an unambiguous association between the measurements and the targets at time k

$$\Theta = \bigcap_{j=1}^{m} \theta(j,t_j) \tag{16}$$

where

- $\theta(j,t_j)$ is the event that measurement j originates from target t_j.
- t_j is the index of the target to which measurement j is associated in the event under consideration.

The event Θ can also be represented by the matrix

$$\Omega_\Theta = [\omega_\Theta(j,t)] \tag{17}$$

consisting of the units in Ω corresponding to the associations in Θ

$$\omega_\Theta(j,t) = \begin{cases} 1 & \text{if the event } \theta(j,t) \text{ is part of } \Theta \\ 0 & \text{otherwise} \end{cases}. \tag{18}$$

Using this, a feasible association event needs to fulfill the following requirements:

1) A measurement can have only one source, i.e.

$$\sum_{t=0}^{N_T} \omega_\Theta(j,t) = 1 \qquad \forall\ j. \tag{19}$$

2) At most one measurement can originate from a target

$$\delta^t_\Theta \triangleq \sum_{j=1}^{m} \omega_\Theta(j,t) \le 1 \qquad t = 1,\ldots,N_T. \tag{20}$$

The binary variable δ^t_Θ is called the target detection indicator since it indicates whether a measurement is associated to a target t or not in event Θ. It is also convenient to define two more binary variables

$$\tau_\Theta(j) \triangleq \sum_{t=1}^{N_T} \omega_\Theta(j,t) \tag{21}$$

$$\phi_\Theta \triangleq \sum_{j=1}^{m} [1 - \tau_\Theta(j)] \tag{22}$$

where $\tau_\Theta(j)$ is the measurement association indicator to indicate if measurement j is associated to a target or not, and ϕ_Θ is the number of false (unassociated) measurements in event Θ.

3.3. Modified JPDAF with a Wake Model

The joint association event probabilities are derived using Bayes' formula

$$\begin{aligned} P\{\Theta_k \mid Z^k\} &= P\{\Theta_k \mid Z_k, m_k, Z^{k-1}\} \\ &= \frac{1}{c} p[Z_k \mid \Theta_k, m_k, Z^{k-1}] P\{\Theta_k \mid Z^{k-1}, m_k\} \\ &= \frac{1}{c} p[Z_k \mid \Theta_k, m_k, Z^{k-1}] P\{\Theta_k \mid m_k\} \end{aligned} \tag{23}$$

where c is a normalizing constant. In the last line of the above equation the irrelevant conditioning term Z^{k-1} has been omitted. The pdf of the measurements in (23) is derived by assuming that the states of the targets, conditioned on the past observations, are mutually independent

$$p[Z_k \mid \Theta_k, m_k, Z^{k-1}] = \prod_{j=1}^{m_k} p[z_k(j) \mid \theta_k(j,t_j), Z^{k-1}]. \tag{24}$$

Measurements not associated to a target are assumed either from the wakes with pdf $p_W(z_k(j))$ with a priori probability P_W, or from uniformly distributed noise/clutter with a priori probability $(1 - P_W)$. Defining V_k as the volume of the joint validation gate, the pdf of a measurement given its origin is

$$\begin{aligned} &p[z_k(j) \mid \theta_k(j,t_j), Z^{k-1}] \\ &\quad = \begin{cases} \mathcal{N}[z_k(j); \hat{z}^{t_j}_{k|k-1}, S^{t_j}_k] & \text{if} \quad \tau_{\Theta_k}(j) = 1 \\ P_W \dfrac{p_W(z_k(j))}{P_{GW}} + (1 - P_W)\dfrac{1}{V_k} & \text{if} \quad \tau_{\Theta_k}(j) = 0 \end{cases} \end{aligned} \tag{25}$$

where $\hat{z}^{t_j}_{k|k-1}$ is the predicted measurement for target t_j with associated innovation covariance $S^{t_j}_k$. The constant P_{GW} is used for restricting $p_W(z_k(j))$ to the joint validation region, and has an analytical expression derived in Appendix A. Using the above equation, (24) can be

written as

$$p[Z_k \mid \Theta_k, m_k, Z^{k-1}] = \prod_{j=1}^{m_k} \{\mathcal{N}[z_k(j); \hat{z}_{k|k-1}^{t_j}, S_k^{t_j}]\}^{\tau_\Theta(j)} \times \left\{ P_W \frac{p_W(z_k(j))}{P_{GW}} + (1 - P_W)\frac{1}{V_k} \right\}^{1-\tau_\Theta(j)}. \quad (26)$$

Next, the last term in (23) will be derived. Let δ_Θ be the vector of detection indicators corresponding to event Θ_k

$$\delta_\Theta = [\delta_\Theta^1, \ldots, \delta_\Theta^{N_T}]. \quad (27)$$

The vector δ_Θ and the number of false measurements ϕ_Θ follow from the event Θ under consideration. Using the definition of conditional probabilities [20, p. 28], this yields

$$P\{\Theta_k \mid m_k\} = P\{\Theta_k, \delta_\Theta, \phi_\Theta \mid m_k\} = P\{\Theta_k \mid \delta_\Theta, \phi_\Theta, m_k\} P\{\delta_\Theta, \phi_\Theta \mid m_k\}. \quad (28)$$

The first term in (28) is obtained using combinatorics:

1) In event Θ_k there are assumed $m_k - \phi_\Theta$ targets detected.

2) The number of events Θ_k, where the same targets are detected, is given by the number of ways of associating $m_k - \phi_\Theta$ measurements to the detected targets from a set of m_k measurements.

By assuming each such event a priori equally likely, one has

$$P\{\Theta_k \mid \delta_\Theta, \phi_\Theta, m_k\} = \frac{1}{{}_{m_k}P_{m_k-\phi_\Theta}} = \frac{\phi_\Theta!}{m_k!}. \quad (29)$$

The last term in (28) is, assuming δ and ϕ independent,

$$P\{\delta_\Theta, \phi_\Theta \mid m_k\} = \prod_{t=1}^{N_T} (P_{\mathrm{D}}^t)^{\delta_\Theta^t} (1 - P_{\mathrm{D}}^t)^{1-\delta_\Theta^t} \mu_F(\phi_\Theta) \quad (30)$$

where P_{D}^t is the detection probability of target t and $\mu_F(\phi_\Theta)$ is the prior pmf of the number of false measurements. The indicators δ_Θ^t have been used to select the probabilities of detection and no detection events according to the event Θ_k under consideration. Combining (29) and (30) into (28) yields the prior probability of a joint association event

$$P\{\Theta_k \mid m_k\} = \frac{\phi_\Theta!}{m_k!} \prod_{t=1}^{N_T} (P_{\mathrm{D}}^t)^{\delta_\Theta^t} (1 - P_{\mathrm{D}}^t)^{1-\delta_\Theta^t} \mu_F(\phi_\Theta). \quad (31)$$

The pmf of the number of false measurements $\mu_F(\phi)$ can, as in the case of the PDA, have two versions, parametric or nonparametric.

1) Parametric JPDA uses a Poisson pmf

$$\mu_F(\phi) = e^{-\lambda V} \frac{(\lambda V)^\phi}{\phi!} \quad (32)$$

which requires the spatial density λ of the false measurements.

2) Nonparametric JPDA uses a diffuse prior

$$\mu_F(\phi) = \epsilon \qquad \forall\ \phi \quad (33)$$

which does not require the parameter λ.

Using the nonparametric model and combining (31) and (26) into (23) yields the joint association event probabilities

$$P\{\Theta_k \mid Z^k\} = \frac{\phi_\Theta!}{c} \prod_{t=1}^{N_T} (P_{\mathrm{D}}^t)^{\delta_\Theta^t} (1 - P_{\mathrm{D}}^t)^{1-\delta_\Theta^t} \times \prod_{j=1}^{m_k} \{\mathcal{N}[z_k(j); \hat{z}_{k|k-1}^{t_j}, S_k^{t_j}]\}^{\tau_\Theta(j)} \times \left\{ P_W \frac{p_W(z_k(j))}{P_{GW}} + (1 - P_W)\frac{1}{V_k} \right\}^{1-\tau_\Theta(j)} \quad (34)$$

where the constants ϵ and $m_k!$ are brought into the normalization constant c. For comparison, the joint association event probabilities derived in [3, p. 318] for the standard JPDAF is

$$P\{\Theta_k \mid Z^k\} = \frac{\phi_\Theta! \cdot V_k^{-\phi_\Theta}}{c} \prod_{t=1}^{N_T} (P_{\mathrm{D}}^t)^{\delta_\Theta^t} (1 - P_{\mathrm{D}}^t)^{1-\delta_\Theta^t} \times \prod_{j=1}^{m_k} \{\mathcal{N}[z_k(j); \hat{z}_{k|k-1}^{t_j}, S_k^{t_j}]\}^{\tau_\Theta(j)} \quad (35)$$

where the third line in (34) is replaced by $V_k^{-\phi_\Theta}$. As for the modified PDAF, (34) reduces to (35) in the limit as P_W goes to zero. Finally, marginal association probabilities are obtained by summing over all the joint association events in which the marginal event of interest occurs

$$\beta_k^t(j) \triangleq P\{\theta_k(j,t) \mid Z^k\} = \sum_{\Theta_k} P\{\Theta_k \mid Z^k\} \omega_\Theta(j,t) \quad (36)$$

$$\beta_k^t(0) \triangleq 1 - \sum_{j=1}^{m_k} \beta_k^t(j). \quad (37)$$

By using these association probabilities in (8), the state estimation equations are exactly the same as in the PDAF, (5)–(11).

3.4. Modified JPDACF

The state estimation above is based on the assumption that the targets, conditioned on the past observations, are mutually independent. When measurements

are inside the validation gates for two or more targets at the same time, we say that the targets are "sharing" measurements. For targets that share measurements for several sampling times, a dependence of their estimation error ensues, and this can be taken into account by calculating the resulting error correlations [7]. The resulting JPDACF algorithm [3, pp. 328–329] does the filtering in a coupled manner, yielding a covariance matrix with cross-covariances that reflect the correlation between the targets' state estimation errors. The effectiveness of the JPDACF approach in combination with the IMM was demonstrated on splitting targets in [2]. This JPDACF approach does not account for situations with partial target detections since the association events where all targets are detected are not separated from events where only some of them are detected. The association events need to be separated in groups where the group member events have the same vector of detection indicators δ_Θ, see (27). This situation was accounted for in the CPDA filter, derived in [9], where the CPDA in combination with hypothesis pruning was developed to avoid track coalescence. In our simulations, however, the CPDA approach did lead to numerical problems in the covariance calculations. An equivalent solution to the CPDA, but where the covariance calculation is in a symmetrical form, is therefore developed and used in this paper to avoid numerical problems. The modified JPDACF accounting for partial target detections and the presence of wakes, is derived next.

Assuming only two targets, the stacked state vector and its associated covariance are denoted as

$$\hat{x}^S_{k|k-1} = \begin{bmatrix} \hat{x}^1_{k|k-1} \\ \hat{x}^2_{k|k-1} \end{bmatrix} \quad \text{and} \quad P^S_{k|k-1} = \begin{bmatrix} P^1_{k|k-1} & P^{12}_{k|k-1} \\ P^{21}_{k|k-1} & P^2_{k|k-1} \end{bmatrix} \tag{38}$$

where $P^{12}_{k|k-1}$ is the cross-covariance between target 1 and 2. This cross-covariance will be zero before these targets become coupled, i.e., start to share measurements. The updated state estimate is

$$\hat{x}^S_{k|k} = \hat{x}^S_{k|k-1} + \sum_{\Theta_k} P\{\Theta_k \mid Z^k\} I^x_\Theta W^S_k I^z_\Theta \nu^S_k(\Theta) \tag{39}$$

where

$$\nu^S_k(\Theta) = z^S_k(\Theta) - \hat{z}^S_{k|k-1} \tag{40}$$

$$z^S_k(\Theta) = \begin{bmatrix} z_k(j_1(\Theta)) \\ z_k(j_2(\Theta)) \end{bmatrix} \tag{41}$$

$$\hat{z}^S_{k|k-1} = H^S \hat{x}^S_{k|k-1} \tag{42}$$

and $j_t(\Theta_k)$ is the index of the measurement associated with target t in the event Θ_k at time k. The filter gain in (39) is

$$W^S_k = P^S_{k|k-1} H^{S^T} [H^S P^S_{k|k-1} H^{S^T} + R^S]^{-1} \tag{43}$$

where

$$H^S = \begin{bmatrix} H^1 & 0 \\ 0 & H^2 \end{bmatrix} \quad \text{and} \quad R^S = \begin{bmatrix} R^1 & 0 \\ 0 & R^2 \end{bmatrix}. \tag{44}$$

The matrices I^x_Θ and I^z_Θ in (39) are used to choose only the innovation from the target(s) that are detected, given by the detection indicator in (20), such that

$$I^x_\Theta = \begin{bmatrix} \delta^1_\Theta I_{n_x} & 0 \\ 0 & \delta^2_\Theta I_{n_x} \end{bmatrix} \tag{45}$$

$$I^z_\Theta = \begin{bmatrix} \delta^1_\Theta I_{n_z} & 0 \\ 0 & \delta^2_\Theta I_{n_z} \end{bmatrix}. \tag{46}$$

Here, I_{n_x} and I_{n_z} are $n_x \times n_x$ and $n_z \times n_z$ identity matrices, where n_x and n_z are the dimensions of a single target state vector and a single target measurement, respectively. Notice that if a target is undetected in the joint association event Θ_k under consideration, the corresponding part of the innovation vector needs to be set to zero even though I^x_Θ is multiplied to the Kalman gain W^S_k. This is accomplished by I^z_Θ.

The updated stacked covariance $P^S_{k|k}$, conditioned on all measurements up to time k, Z^k, is derived in Appendix B and yields

$$\begin{aligned} P^S_{k|k} = {} & \sum_{\Theta_k} P\{\Theta_k \mid Z^k\} \\ & \times \{I^x_\Theta W^S_k I^z_\Theta (\nu^S_k(\Theta)\nu^S_k(\Theta)^T + R^S) I^z_\Theta W^{S^T}_k I^x_\Theta \\ & \quad + (I - I^x_\Theta W^S_k I^z_\Theta H^S) P^S_{k|k-1} (I - I^x_\Theta W^S_k I^z_\Theta H^S)^T\} \\ & - \left(\sum_{\Theta_k} P\{\Theta_k \mid Z^k\} I^x_\Theta W^S_k I^z_\Theta \nu^S_k(\Theta) \right) \\ & \times \left(\sum_{\Theta_k} P\{\Theta_k \mid Z^k\} I^x_\Theta W^S_k I^z_\Theta \nu^S_k(\Theta) \right)^T. \end{aligned} \tag{47}$$

The joint association event probabilities $P\{\Theta_k \mid Z^k\}$ are calculated as for the decoupled filter in Section 3.3, and the prediction step is as in (5), but with stacked state and covariance.

4. MULTISENSOR TRACKING

The best performance in multisensor data fusion is achieved using centralized configurations where all measurements are transmitted from the local sensors to a fusion center.[1] Primarily due to the bandwidth constraints in real systems, the centralized configuration is sometimes not feasible because its requirement to transmit all measurement information to a fusion center. This is the motivation for the interest in decentralized track-

[1] It is assumed that the sensors are properly registered and have no biases.

ing, with track-to-track association followed by track fusion, which has been compared to centralized tracking in [10], [11]. To make the centralized tracking more feasible for real systems, the measurement data can be compressed in the local sensors before they are transmitted [12]. When the measurements are transmitted to a fusion center in the centralized tracking, there are two different schemes for the way the state is updated. In parallel filtering the measurements from all sensors (if synchronized) are taken into account at the same time. The other alternative is sequential filtering where measurements from each sensor is processed one sensor at a time. The first sensor updates the state (and covariance) based on predictions from the previous time step as in a single-sensor algorithm. Then, this new updated state is used as a zero-time prediction to update with the measurements from the second sensor and so on. In [19] the sequential and parallel filtering schemes are compared in a multisensor JPDAF approach, and it is shown that sequential filtering is less computationally expensive as the number of sensors increases. According to [19], the sequential method yields better tracking performance on the average when data association is needed. This is primarily due to the fact that better filtered estimates are available after processing each sensor's data.

Another problem regarding multisensor systems is the positioning of the sensors, where there are several aspects to consider:

- The sensors' joint ability to cover the required area.
- The sensor specifications.
- The most likely target locations and trajectories.
- The possibility of tracking the targets from various view angles.

These factors, among others, have to be considered separately and in light of the main purpose of each specific tracking problem.

5. SIMULATIONS AND RESULTS

In this section the data association methods described previously (PDAF, Modified PDAF, JPDAF, Modified JPDAF and Modified JPDACF) are compared in four different multitarget simulation scenarios in the presence of wakes. These simulations consider an underwater surveillance system with active sonar sensors and scuba divers as the targets. The wakes are generated by the air bubbles from the divers. Results are shown using two sensors, working both as independent single sensors and together in a centralized tracking system. When the filters discussed above are used in multisensor (MS) situations in the centralized tracking configuration, they will be denoted as MSPDAF, Modified MSPDAF, MSJPDAF, Modified MSJPDAF and Modified MSJPDACF.

5.1. Simulation Scenarios

The four simulation scenarios are shown in Fig. 4, and are in the sequel denoted as:

1) *Crossing scenario*: The targets are starting in positions $(25, 32.5)$ m and $(25, 67.5)$ m with speed 1 m/s and course according to the trajectory crossing angle $\gamma = 20^\circ$, see Fig. 4. The nearly straight trajectories are crossing the 200 s run midway. In [22] a similar scenario with varying trajectory crossing angle $\gamma = [5^\circ, 6^\circ, \ldots, 30^\circ]$ is simulated for a single sensor, showing significant reduction of track loss for the modified filters.

2) *Parallel scenario*: The targets are starting in positions $(25, 40)$ m and $(25, 60)$ m with speed 1 m/s and course according to the trajectory crossing angle $\gamma = 15^\circ$. When the distance between the targets is less than 3 m, their velocities are both set to $[1, 0]$ m/s, creating parallel trajectories with 3 m spacing. Then, after 130 s they separate in the same way as they joined each other.

3) *Sequential scenario*: The targets are starting in positions $(22.5, 40)$ m and $(27.5, 60)$ m with speed 1 m/s and course according to the trajectory crossing angle $\gamma = 15^\circ$. When the distance between the targets is less than 0.5 m in the y-direction their velocities are both set to $[1, 0]$ m/s. Since the first target started 5 m behind the second target in the x-direction, they will now move after each other in the same direction with about 5 m spacing. Then, after 130 s they separate in the same way as they joined each other. Note that Target 1 is moving inside the wake created by Target 2 before they separate.

4) *Meeting scenario*: The targets are starting in positions $(25, 50)$ m and $(225, 50)$ m with speed 1 m/s and course directly towards each other. The targets are passing each other without changing course. Note that both targets are moving inside the wake of the other one after the passing.

5.2. Simulation Setup

Two sensors, with the same specifications, are located in the positions $(0, 0)$ m and $(250, 100)$ m respectively. The sensors have 180° field of view with resolution about 0.7° in bearing (256 non-overlapping beams) and 0.2 m in range. Their maximum range of 250 m is assumed large enough to cover the targets throughout the 200 s long runs, consisting of 200 scans with sampling period $T = 1$ s. For both targets a two-dimensional direct discrete time nearly constant velocity model [4] is used in (1) and (2):

$$F = \begin{bmatrix} 1 & T & 0 & 0 \\ 0 & 1 & 0 & 0 \\ 0 & 0 & 1 & T \\ 0 & 0 & 0 & 1 \end{bmatrix} \qquad H = \begin{bmatrix} 1 & 0 & 0 & 0 \\ 0 & 0 & 1 & 0 \end{bmatrix} \tag{48}$$

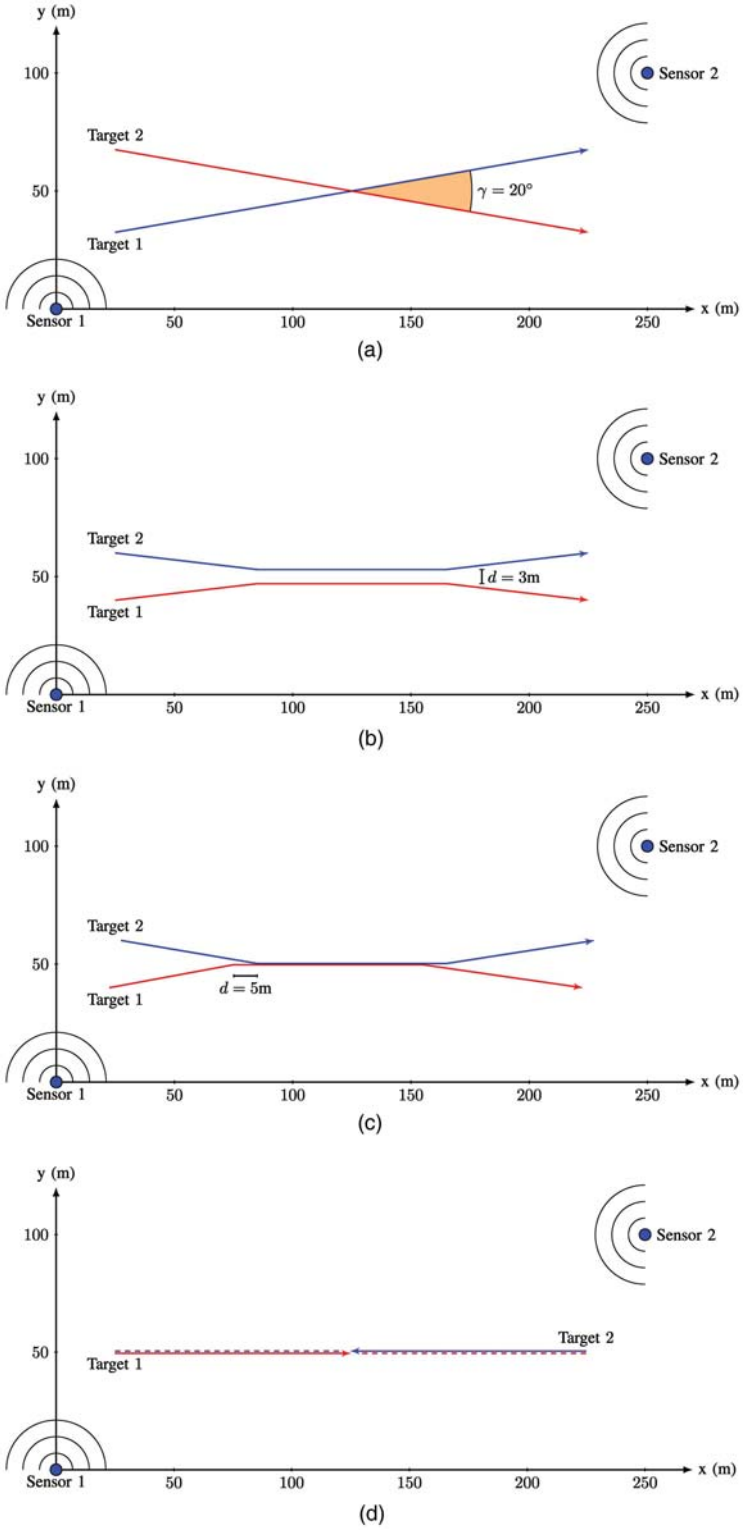

Fig. 4. Simulation scenarios of two targets observed by two sensors. Four different scenarios are shown. (a) Scenario 1: Crossing trajectories with trajectory crossing angle $\gamma = 20°$. (b) Scenario 2: Parallel trajectories where the targets are moving side by side with spacing $d = 3$ m. (c) Scenario 3: Sequential trajectories where Target 1 is moving behind in the wake created by Target 2, with spacing $d = 5$ m. (d) Scenario 4: Meeting trajectories where the targets are moving towards each other, and passing each other inside the wake of the other target.

$$R_c = \begin{bmatrix} \sigma_x^2 & \sigma_{xy}^2 \\ \sigma_{xy}^2 & \sigma_y^2 \end{bmatrix} \qquad R_p = \begin{bmatrix} \sigma_r^2 & 0 \\ 0 & \sigma_\psi^2 \end{bmatrix} \tag{49}$$

$$Q = \begin{bmatrix} \frac{1}{4}T^4 & \frac{1}{2}T^3 & 0 & 0 \\ \frac{1}{2}T^3 & T^2 & 0 & 0 \\ 0 & 0 & \frac{1}{4}T^4 & \frac{1}{2}T^3 \\ 0 & 0 & \frac{1}{2}T^3 & T^2 \end{bmatrix} \sigma_p^2. \tag{50}$$

TABLE I
Specification of Parameters

Parameter	Value	Specification
T	1.0 s	Sampling period
P_{D}	0.7	Detection probability
P_G	0.99999	Gate probability
P_W	0.9	Wake probability
P_{FA}	0.001	False alarm probability
$\sigma_p^2(\mathrm{s})$	$(0.001\ \mathrm{m/s^2})^2$	Process noise (simulation model)
$\sigma_p^2(\mathrm{f})$	$(0.05\ \mathrm{m/s^2})^2$	Process noise (filter model)
σ_r^2	$(0.2\ m)^2$	Measurement noise (range)
σ_ψ^2	$(3.5 \cdot 10^{-3}\ \mathrm{rad})^2$	Measurement noise (bearing)
N	256×1250	Number of resolution cells
S	180°, 250 m range	Sensor coverage area
M	250×40 m	Measurement generation area
W	5×30 m	Wake area
V_S	98174 $\mathrm{m^2}$	Volume of S
V_M	10000 $\mathrm{m^2}$	Volume of M
V_W	150 $\mathrm{m^2}$	Volume of W
$\lambda_{\mathrm{clutter}}$	16.3	Expected number of correlated clutter measurements

The parameters in (48)–(50) and other simulation design parameters are given in Table I.

Originally, the position measurements are in polar coordinates (r, ψ) with (time invariant) measurement noise covariance R_p, but are transformed to Cartesian coordinates (x, y) with corresponding measurement noise covariance R_c using the standard conversion [4, pp. 397–399]. This results in a purely linear model so that a Kalman filter can be used in the tracking algorithm. The measurement noise matrix R_p is calculated assuming a uniformly distributed position error inside the resolution cell. Hence, the variance of the uniformly distributed error is given by the resolution, and this variance is heuristically used as the variance in the Gaussian distributed R_p

$$\sigma_r^2 = \frac{0.2^2}{12}\ \mathrm{m^2} \qquad \text{and} \qquad \sigma_\psi^2 = \frac{(\pi/256)^2}{12}\ \mathrm{rad^2}. \tag{51}$$

Due to the high resolution in range (0.2 m), the targets will cover several resolution cells in the range direction, resulting in extended targets. Because of this, the actual range resolution is used as the standard deviation ($\sigma_r = 0.2$ m) instead of the calculation in (51). This modification of σ_r in the simulations seems more reasonable since the targets (scuba divers) are extended in the range direction. To ensure controlled trajectories for the true targets, the added process noise in the simulation model $\sigma_p^2(\mathrm{s}) = (0.001\ \mathrm{m/s^2})^2$ is set low, but not to zero. The process noise in the filter model $\sigma_p^2(\mathrm{f}) = (0.05\ \mathrm{m/s^2})^2$ is set to approximate about 5 cm/s change in the velocity components between each scan.

When the targets are following after each other in the sequential scenario, there will be a problem using the filter modifications as described above. This problem especially affects the target following behind the first target, because there will be wake detections surrounding this target both in front and behind it. If the wake model is used in this situation, the wake-dominated measurements behind the target will get lower weights than the wake-dominated measurements in front. These measurements in front, which originate from the wake of the first target, will mislead the tracker, and the estimated track will speed up until it catches up with the target in front. It is therefore likely that this target will be lost. An approach to prevent this is to only apply the wake model to the target in front, and use a regular data association filter for the target that is following the first one. By handling the two targets separately in two single-target tracking filters, the track of the target behind the first one will have better chance to survive in this hard situation. In the simulations a target following behind another one will therefore not use the wake model if the following criteria are fulfilled:

1) The target is inside the wake area W of the target in front. The wake area W is defined as a rectangle, L_w wide and reaching L_l backwards from the target ($L_w = 5$ m, $L_l = 30$ m).

2) The target is at least 2 m behind the target in front.

3) The difference between the moving direction of the following target and the target in front is less than 10°.

To reduce the computational load, the different versions of the multitarget tracking algorithms are substituted with their analogous single target tracking algorithms as long as targets are not "sharing" measurements. In other words, the standard PDAF is used instead of the JPDAF, and the modified PDAF is used instead of the modified JPDAF and JPDACF when the targets are apart. The multisensor (MS) filters are treated in the same way, i.e., the MSPDAF is used instead of the MSJPDAF.

5.3. Measurement Generation

The directional information (bearing) in an active sonar is given by the beamforming. Since no beamforming can achieve an ideal directivity pattern, there will be a leakage or scattering of the signal in one beam to the neighboring beams [16, ch. 5.3]. This is also known as the point spread function (psf) [25], and may yield detections from a point target in more than one bearing cell. In [22] the true target-originated measurements are simulated as single point detections, which, as described above, is a simplification of the real world. To generate measurements from the targets and their wakes in this paper, detections from a *real data set* of a scuba diver with an open breathing system are used. The data set consists of 500 scans, and is recorded by an active sonar with the same specifications as the sensors used in the simulations. The diver is swimming in a nearly straight

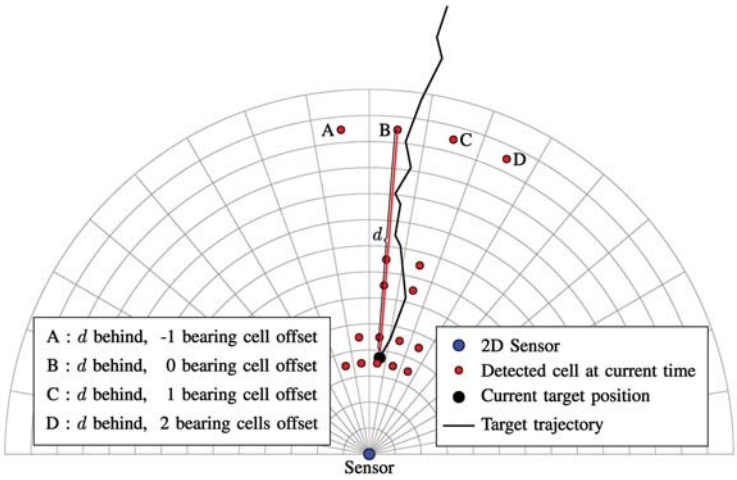

Fig. 5. Illustration of how each detection is specified by using the distance behind the target d and a bearing offset. The bearing offset describes the number of cells in the bearing direction between a detected cell and the cell where the target trajectory passes through, and with the same range as the detected one. As an example, the four detections marked with A, B, C and D are the same distance behind the target, but with offsets -1, 0, 1 and 2 respectively.

line, and its trajectory is estimated mainly by using a modified PDAF [21], but some manual corrections are done to get better position estimates. For each scan a cell averaging–constant false alarm rate (CA-CFAR) detector [15] is used to obtain the detections. The parameters of the CA-CFAR algorithm are the same as in [21], except for the following parameters:

- The average false alarm rate (probability of a false detection in a resolution cell) is set to $P_{\mathrm{FA}} = 0.001$.
- The size of the averaging window used to estimate the local background noise parameter is increased to 51 cells in the range direction due to the increased resolution of the sensors used in this paper.

For each scan, the detections are stored and specified by a distance d behind the true target position and a bearing offset, see Fig. 5. The bearing offset describes the number of cells in the bearing direction between a detected cell and the cell where the target trajectory passes through, and with the same range as the detected one. As an example, the four detections marked with A, B, C and D in Fig. 5 are the same distance behind the target, but with bearing offsets -1, 0, 1 and 2 respectively. Finally, after going through the 500 scans in the *real data set*, this gives 500 different sets of detections of the true target and its wake, where the scattering in the bearing-direction is accounted for. In the simulations the detections originating from the target and its wake are generated by drawing from these 500 sets according to a first order Markov model. If set s was drawn at scan k, the probability of drawing the succeeding set $s+1$ at time $k+1$ is $\pi_{s,s+1} = 0.7$, and the probability of a random drawing $u \in [1,500]$ (uniformly distributed) is $\pi_{s,u} = 1 - \pi_{s,s+1} = 0.3$. The targets' states are generated directly from (1), and with the position and velocity known, the target and wake originated measurements are added.

Another part of the measurements is the clutter or false measurements, and a standard assumption in simulations is that clutter is uniformly distributed in the surveillance area. In this paper the generation of clutter is done in two steps. The first step is under the standard assumption, where the probability of generating a clutter measurement in a resolution cell is $P_{\mathrm{FA}}/2 = 0.005$, uniformly distributed across all cells in range and bearing. The second step is to generate spatially correlated clutter. These measurements are generated from a multimodal Gaussian pdf with equal weights for the different modes. This is an approach to reflect that some areas in the surveillance region yields more clutter, due to, e.g., a rough surface of the sea bed, banks, hills, large stones and other objects that creates variation in the surveillance area. The multimodal Gaussian pdf is regenerated for each run, and the number of modes is drawn as a uniform discrete variable between 1 and 10. The mean of each Gaussian mode is drawn uniformly in the surveillance area, and the covariance matrix is diagonal with standard deviations in the x and y directions drawn as uniform variables between 0 and 10. The number of correlated clutter measurements for each scan is Poisson distributed with parameter $\lambda_{\mathrm{clutter}}$. Denote the coverage area for a sensor as S (180°, 250 m range), and the measurement area covering the full trajectories of the targets as M (250×40 m), with volume V_S and V_M respectively. The Poisson parameter $\lambda_{\mathrm{clutter}}$ is then given by

$$\lambda_{\mathrm{clutter}} = 0.5 P_{\mathrm{FA}} N \frac{V_M}{V_S} \approx 16.3 \tag{52}$$

where P_{FA} is the probability of a false alarm in a resolution cell, and N is the number of resolution cells in S. Hence, in average there will be 16.3 correlated clutter measurements in M for each scan. An example of all measurements in one time frame for the crossing scenario is given in Fig. 6. Notice that the detections

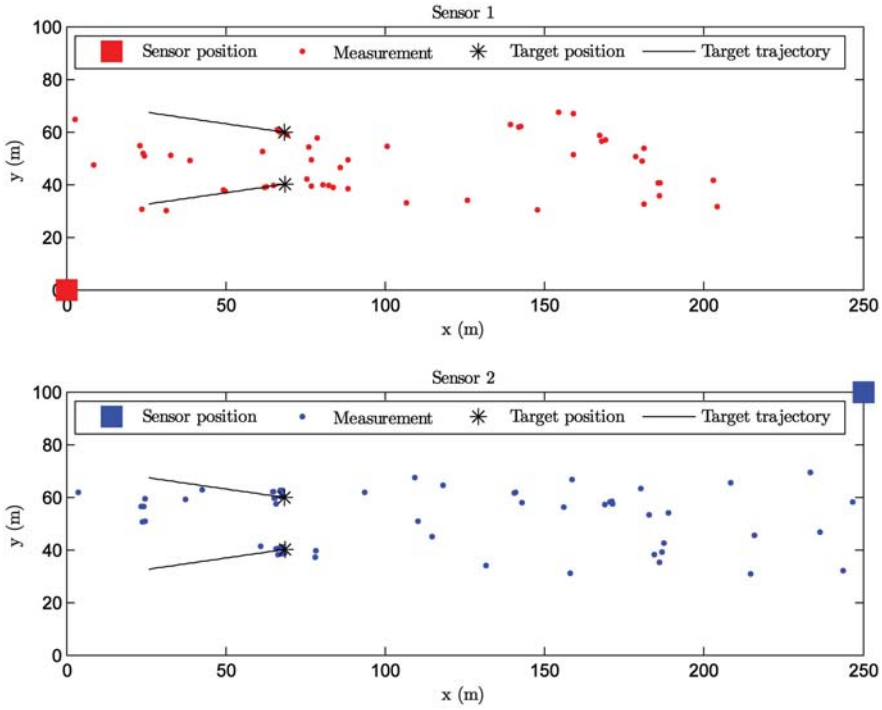

Fig. 6. Snapshot of all detections/measurements at Sensor 1 and Sensor 2 during a run in the crossing scenario.

of the targets are more spread out sideways in Sensor 2 than in Sensor 1. At this time the targets are closer to Sensor 1 than Sensor 2, and they are therefore better resolved by Sensor 1. The targets are also moving towards Sensor 2, and because of the scattering of the signal to the neighboring beams, the detections will be spread out more sideways from the direction of motion. Also notice how in some places the detections are located in groups due to the non-uniform spatial distribution of the clutter measurements. It is also possible that a target can be undetected, which is the case for the lower target at Sensor 1 in Fig. 6.

5.4. Track Formation and Termination

As can be seen in Fig. 6, the targets are often determined by a cluster of detections rather than a single point detection. In the simulations the tracks are initialized by two-point differencing [4, p. 247] of the cluster centroids from succeeding scans. The reason for this is to avoid confusion due to the many possibilities of two-point differencing that could have been set up among the point detections from one single target. The clustering method of the single point detections is described in [21], and is based on mathematical morphology [23]. Any successive pair of clusters within a maximum distance based on target maximum motion parameters and cluster measurement noise variances initiates a preliminary track. For the motion parameters, a maximum distance $d_{\max} = 1$ m together with the process noise matrix Q in (2) is used. The measurement noise for the clusters is computed from the different cells included in the cluster as a Gaussian mixture [4, pp. 55–56]. A preliminary track has to receive measurements for a minimum of 4 time steps during the first 6 scans to become a confirmed track. This is also referred to as a "4/6" logic-based track formation procedure. Note that the clustering method is only used for the two-point differencing in the track initialization.

In the centralized tracking the multisensor filtering is described in Section 4, first updating with measurements from Sensor 1 and then with measurements from Sensor 2 in a sequential updating scheme. The track initialization in the centralized tracking algorithm is based on measurements that also contain velocity information. First, the two-point differencing is used at Sensor 1 to make an initial state. Then, the two-point differencing is used at Sensor 2, but these initial states are now used as measurements (including both position and velocity) to update the initial state from Sensor 1. The updating is done as in a regular PDAF, but since these measurements are formed by two-point differencing of cluster centroids from succeeding scans, they will not have the same measurement noise, yielding a varying innovation covariance (S_k in (6)). The innovation covariance is normally used to form the measurement validation gate in the PDAF, but in this case a fixed matrix

$$S_{\text{fix}} = \begin{bmatrix} \sigma^2_{\text{pos}} & 0 & 0 & 0 \\ 0 & \sigma^2_{\text{pos}} & 0 & 0 \\ 0 & 0 & \sigma^2_{\text{vel}} & 0 \\ 0 & 0 & 0 & \sigma^2_{\text{vel}} \end{bmatrix} \tag{53}$$

is used instead of the non-constant innovation covariance to form a constant measurement validation gate.

The values used in S_{fix} is set based on the assumption that the standard deviation for these measurements are about 1 m for the position elements, and 0.5 m for the velocity elements ($\sigma_{\text{pos}} = 1$ m and $\sigma_{\text{vel}} = 0.5$ m).

In the modified filters, the wake assumption also affects the track initialization in the way that measurements inside the wake area W (defined in Section 5.2) are excluded in the initialization procedure.

To terminate a track one of the following events (termination events) must occur:

1) The estimated speed is outside the interval $[v_{\min}, v_{\max}]$, where $v_{\min} = 0.1$ m/s and $v_{\max} = 3$ m/s.
2) The estimate moves more than 5 m between two scans.
3) The position state estimation variance exceeds $\sigma^2_{\text{pos max}}$, where $\sigma^2_{\text{pos max}} = 50$ m^2.
4) There are no validated measurements received in a track within 5 successive scans.
5) The track is closer than $d_{\min}$ to another older track during 10 succeeding scans, where $d_{\min} = 0.5$ m.

These track termination criteria are adopted rather than using more rigorous methods, such as the joint version of the IPDAF [17], because of their sensitivity to inaccurate estimates of the clutter density. In real sensor measurements, the signal is often scattered resulting in more than one target-originated detection. This will increase the clutter density resulting in an unrealistic low probability for the track to survive. This may be solved by the use of clustering, but for targets in the presence of wakes it is undesirable to blend the wake-originated detections together with the target-originated ones. The above termination criteria are more strict than those used in [21] due to the higher sensor resolution used in this paper.

5.5. Performance Analysis

The performance evaluation of a multitarget tracking system is always a difficult problem, and the quality of the results is difficult to quantify in terms of a few variables. When the evaluation is based on real data, where not all parameters are known, this problem becomes even harder. The results also depend on the simulation scenarios, and the performance of the JPDAF may, according to [13], show large local maxima and minima as a function of scenario parameters. However, by considering the basic scenarios described above and using a relatively large set of measures of performance (MOP), a certain amount of meaningful information should be obtained. The MOP considered are the following:

1) The percentage of lost tracks among all true tracks.
2) The percentage of swapped tracks among all true tracks (measured only when the targets are closer than 10 m).
3) The average fraction of each trajectory's total duration where the target is tracked (by a true track).
4) The average life length of a true track relative to its true target's life length.
5) The average time for target acquisition.
6) The number of false tracks per scan.
7) The average life length of a false track.
8) The position RMS error.

This section describes how these MOP are obtained before the corresponding results, based on 500 Monte Carlo runs for each of the four given scenarios, are shown. At a given time k there might exist several tracks, but for each target, at most one of them can be defined as true. The rest of the tracks are therefore by definition false. A track is first defined as true if the position estimation error is less than 1 m during the next 5 scans, and at the same time there are no other true track associated to the target. If there is more than one track fulfilling these requirements at the same time, the track with lowest average position estimation error during these 5 scans is defined as the true one. The true track will stay as such until either the position estimation error exceeds 5 m, or the position estimation error associated to a neighboring target is less than 1 m during the next 5 scans. In both situations the track will be declared as lost, but in the latter case it will also be defined as a swapped track.

1) *The percentage of lost tracks among all true tracks*: In Fig. 7 the percentage of lost tracks is shown. The standard filters (PDAF and JPDAF) have the highest track loss percentage, and the JPDAF shows no improvement compared to the PDAF. The modified single target tracking algorithm (PDAF) performs better than the standard filters, but the best performance is achieved with the modified JPDAF and JPDACF. The difference between the standard filters and the modified PDAF is largest in the meeting and crossing scenarios where the targets are close to each other during a short time. When the targets stay together for a longer period of time, the modified PDAF is not significantly better than the standard filters because it does not account for the neighboring target and its wake like the modified JPDAF and JPDACF do. Also notice that there is almost no difference between the decoupled and coupled modified JPDAF, which indicates that the correlation between the targets' estimation errors is insignificant.

In the different scenarios considered the best performance is achieved for the meeting scenario. This is maybe a bit surprising since the density of the joint wake model after the passing is lowest between the targets, the area opposite to their moving direction. However, the high wake density in the whole joint validation region will at the same time give more confidence in the predicted target motion than the measurements. Because of this, and the fact that the velocities of the two targets are totally opposite to each other, the tracks will be less affected by the false measurements. The percentage of the lost tracks in the crossing scenario is the next best, and the good performance in both the meeting and crossing

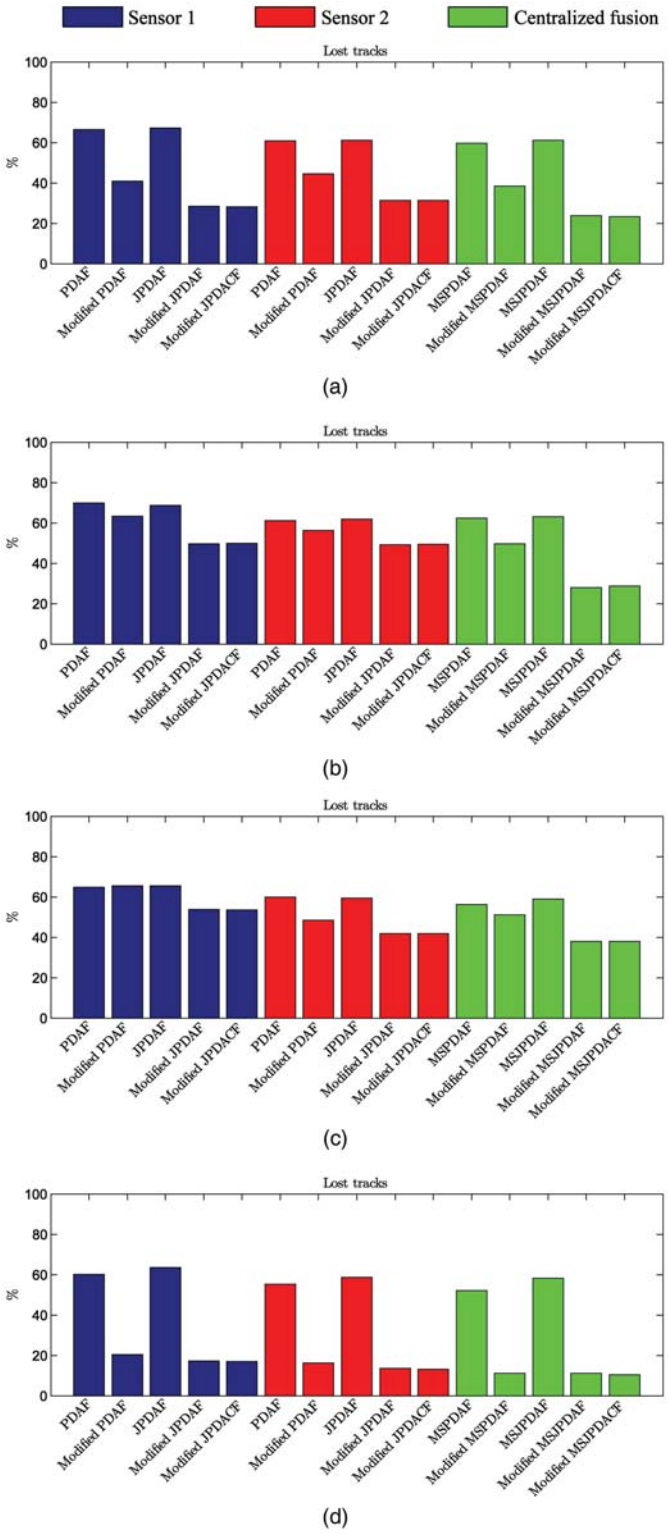

Fig. 7. Average percentage of lost tracks in the four simulation scenarios. (a) Scenario 1: Crossing trajectories. (b) Scenario 2: Parallel trajectories. (c) Scenario 3: Sequential trajectories. (d) Scenario 4: Meeting trajectories.

scenarios is as expected since the targets are only close to each other a short time. In these scenarios the results from the single sensor filters are almost as good as from the multisensor filters in the centralized tracking. This is not true for the parallel scenario where the performance is significantly improved by fusing the sensors' data in the modifed MSJPDAF and MSJPDACF. In this scenario the targets are separated by only 3 m, which is close to the limit for having multiple targets in a single resolution cell (unresolved targets). By using two sensors in this situation, Sensor 1 resolves the targets relatively good in the beginning of the run, and Sen-

sor 2 does the same at the end of the run. Because of this, the fusion of these two sensors data improves the performance significantly.

The most difficult scenario is the sequential, where a target is moving behind another target, surrounded by the wake. In this case the centralized tracking performs best, and a track loss under 40% is achieved by the modified MSJPDAF and MSJPDACF. In practice this means that, even in a hard case like this, at least one track will be kept throughout the run.

2) *The percentage of swapped tracks among all true tracks (measured only when the targets are closer than 10 m)*: The percentage of the swapped tracks, shown in Fig. 8, is only measured when the distance between the targets is less than 10 m. The reason for this is to find the percentage of swapping among only the tracks where the two associated targets are close to each other. The swapping is, as expected, highest in the parallel scenario where the tracks are moving in parallel for a longer period of time. In this situation it is easy for a track to switch over to the neighboring target only 3 m away. In the meeting scenario the swapping phenomenon is totally absent for the modified filters, and practically absent for the standard filters (PDAF and JPDAF). The reason for this is the same as discussed under the previous MOP.

The modified PDAF has the most problems, especially in the parallel scenario, since it accounts for its own wake, but does not take into consideration that there is another target in the surrounding area. The standard filters, which do not consider the wakes, are more disposed to turn into their own wake than to swap to the neighboring target. Therefore, even if their track loss is higher, they have a lower swapping percentage than the modified PDAF.

The best performance is achieved by the modified MSJPDAF and MSJPDACF in the centralized tracking. This improvement is most significant in the parallel scenario, where the percentage of swapped tracks are almost halved for the modified MSJPDAF and MSJPDACF compared to the other filters.

3) *The average fraction of each trajectory's total duration where the target is tracked (by a true track)*: In Fig. 9 the average percentage of the tracked part of the trajectories' duration is shown. Also here the modified JPDAF and JPDACF perform best, and by using the modified MSJPDAF or MSJPDACF in the centralized tracking, about 90% of the trajectories are tracked. Notice that the percentage of the tracked trajectory can be very good even with a high track loss percentage if tracks are quickly reacquired after a loss. It is therefore important to consider other MOP to get the total picture.

4) *The average life length of a true track relative to its true target's life length*: In Fig. 10 the average life length (in %) of the true tracks is shown. It is clear that the track length is significantly increased by the modified filters, and most by the modified multitarget tracking filters (JPDAF and JPDACF). The best performance is achieved by the modified filters in the meeting scenario, where the average track length is about 80% of the true target's life length, more than twice as long as for the standard PDAF and JPDAF. The improvement by using multiple sensors is most significant for the modified MSJPDAF and MSJPDACF in the parallel scenario. In this situation the combination of both using the multitarget wake model, and for the targets to be well resolved by at least one sensor all the time throughout the run, is vital. In the sequential scenario the best track length is almost 60% for the same modified multisensor filters. This is due to the fact that when a track is first lost inside the wake of another target in front, it is very hard to reacquire a track on the rear target.

5) *The average time for target acquisition*: In many situations it is important to quickly initiate tracks and reacquire them once lost. Let the time for target acquisition be the time before a track is defined as true either in the beginning of a run or after a track was lost. The average time for target acquisition (or reacquisition) is shown in Fig. 11. For the crossing, the parallel and the meeting scenarios, the modified filters perform slightly better than the standard filters. At the sequential scenario the behavior is different in the way that the standard filters outperform the modified filters. This is due to the assumption that the measurements behind a target originate from a wake and not a target. Therefore, when the target following the target in front is lost, the real target-originated measurements will not be considered for a new track as long as they are inside the wake area W of the target in front.

In the first three scenarios it is harder to initiate/reacquire true tracks at Sensor 2 than for Sensor 1. The reason for this is that tracks are starting close to Sensor 1, and far from Sensor 2, and the detections of the targets (and wakes) will therefore be more spread out in the view of Sensor 2. This can be seen in Fig. 6, and makes it harder to acquire tracks in the two-point differencing of the cluster centroids from succeeding scans.

6) *The average life length of a false track*: As mentioned above, all tracks that are not defined as true, are considered false. The average life length of a false track is shown in Fig. 12, and the performance is almost the same for all filters, with an insignificant tendency for shorter life length of the false tracks in the modified filters.

7) *The number of false tracks per scan*: Another MOP considering the false tracks, is the average number of false tracks per scan, shown in Fig. 13. This number is higher for the standard filters than for the modified ones because the standard filters do not restrict the track formation inside the wake areas behind the targets. Also, there are more false tracks for the centralized tracking due to the fact that this tracking algorithm takes into account false measurements from both sensors.

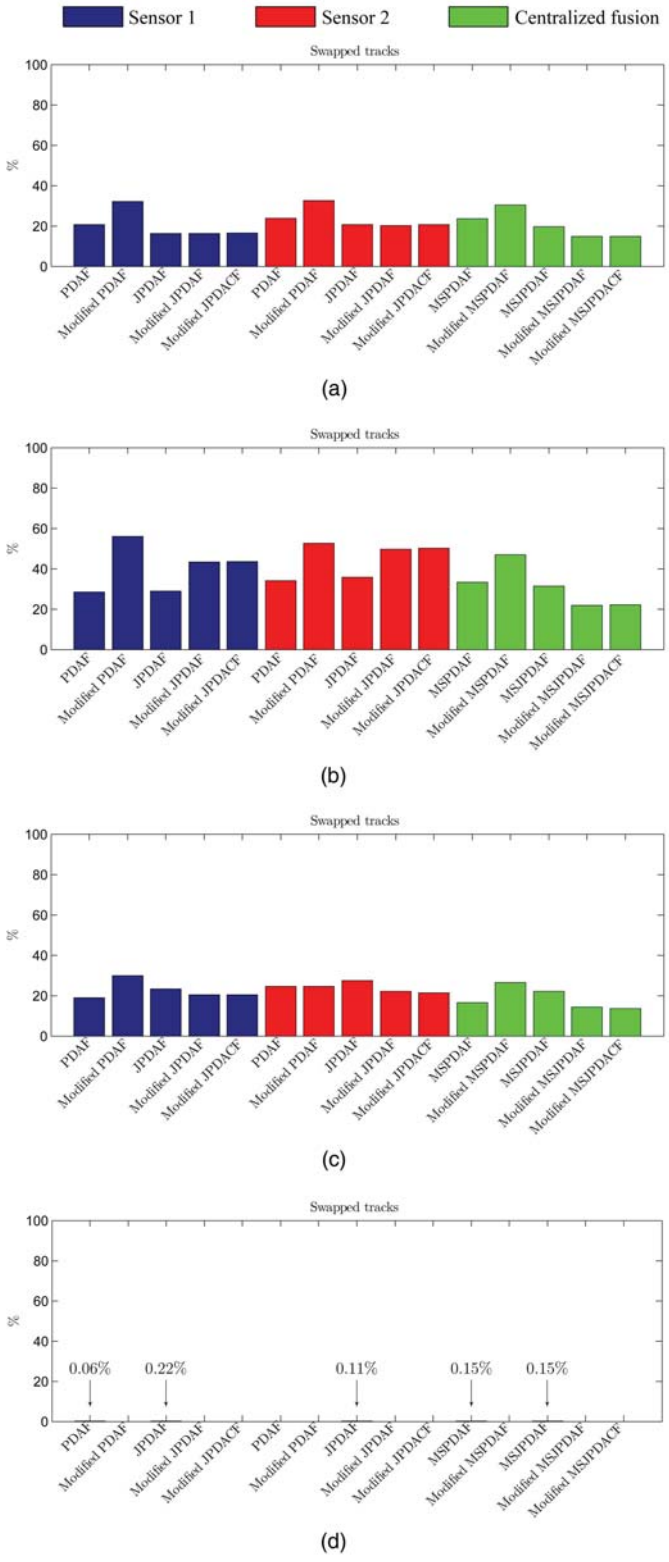

Fig. 8. Average percentage of swapped tracks in the three simulation scenarios. (a) Scenario 1: Crossing trajectories. (b) Scenario 2: Parallel trajectories. (c) Scenario 3: Sequential trajectories. (d) Scenario 4: Meeting trajectories.

8) *The position RMS error*: The last MOP in this analysis is the position RMS error, given in Fig. 14. The RMS error is based only on the true tracks in the simulation scenarios. In all scenarios the position RMS error is larger for the standard filters than for the modified filters. This is because the standard filters do not consider the wake-originated measurements like the modified filters do, and the state estimate is therefore likely to be drawn into the wake. It can also be seen that the RMS error, at least for the modified JPDAF

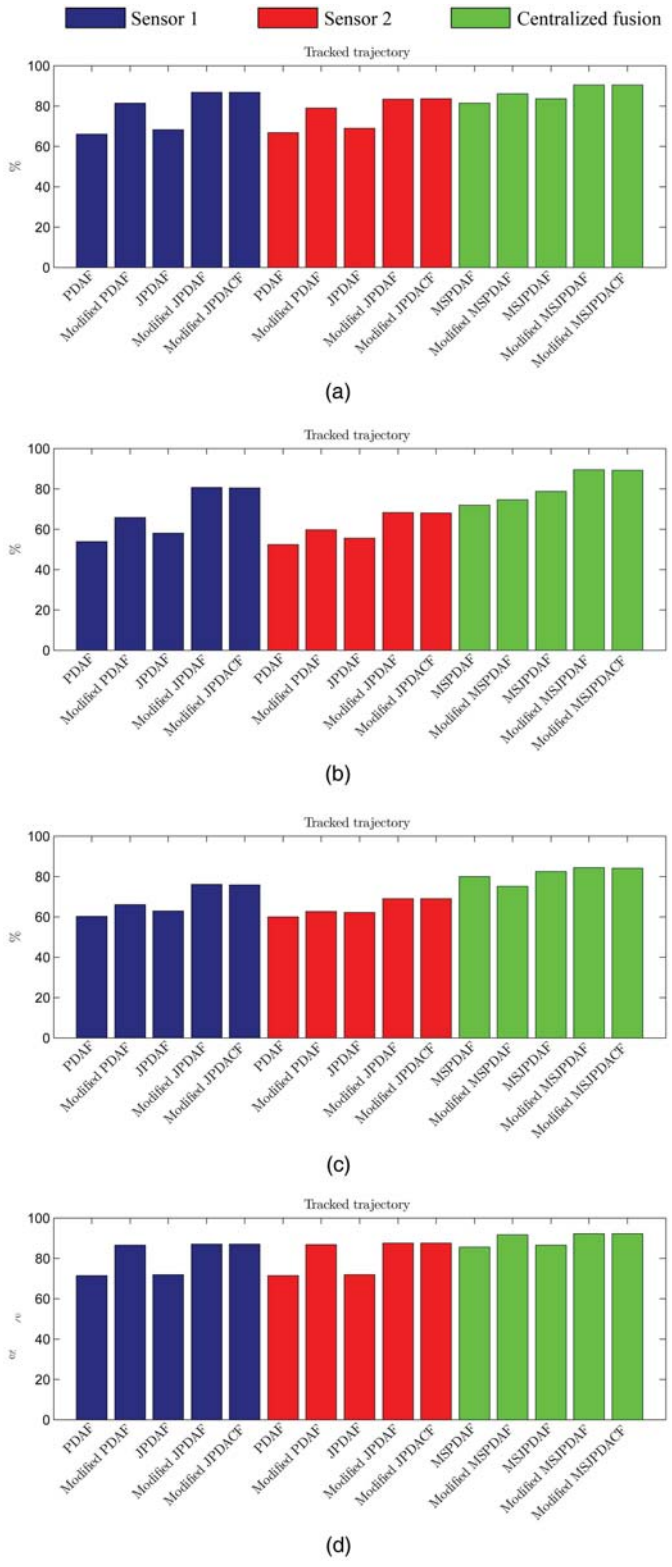

Fig. 9. Average percentage of tracked trajectory in the four simulation scenarios. (a) Scenario 1: Crossing trajectories. (b) Scenario 2: Parallel trajectories. (c) Scenario 3: Sequential trajectories. (d) Scenario 4: Meeting trajectories.

and JPDACF, is slightly reduced in the centralized tracking.

In the two first scenarios (crossing and parallel), the error increases during the periods when the targets are close to each other. For the crossing scenario this is seen as a "jump" in the error when the targets are crossing between 80 s and 120 s. In the parallel scenario, this jump starts at about 60 s and ends at 140 s, which are the period the targets are moving in parallel. In these situations the estimate for one target

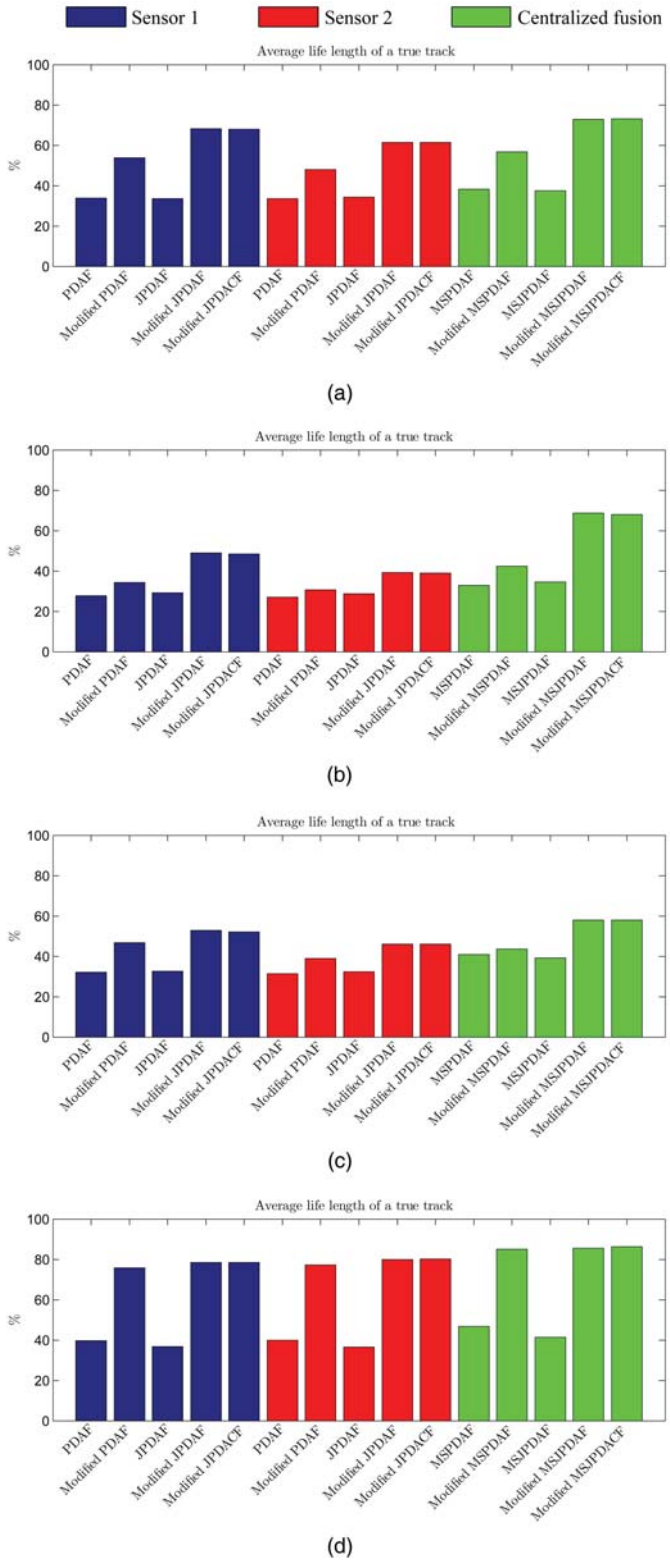

Fig. 10. Average life length of a true track relative to its true target's life length in the four simulation scenarios. (a) Scenario 1: Crossing trajectories. (b) Scenario 2: Parallel trajectories. (c) Scenario 3: Sequential trajectories. (d) Scenario 4: Meeting trajectories.

will be drawn towards the other target, also known as track coalescence [8]. Among the modified filters, this is most problematic for the single target tracking algorithm because it accounts for the wake behind its own target, but has no information about the nearby target which also has a wake behind it. The modified multitarget filters perform similarly, and their RMS errors are almost constant throughout the run.

In the meeting scenario only a small tendency of the jump phenomenon is noticeable shortly after the pass-

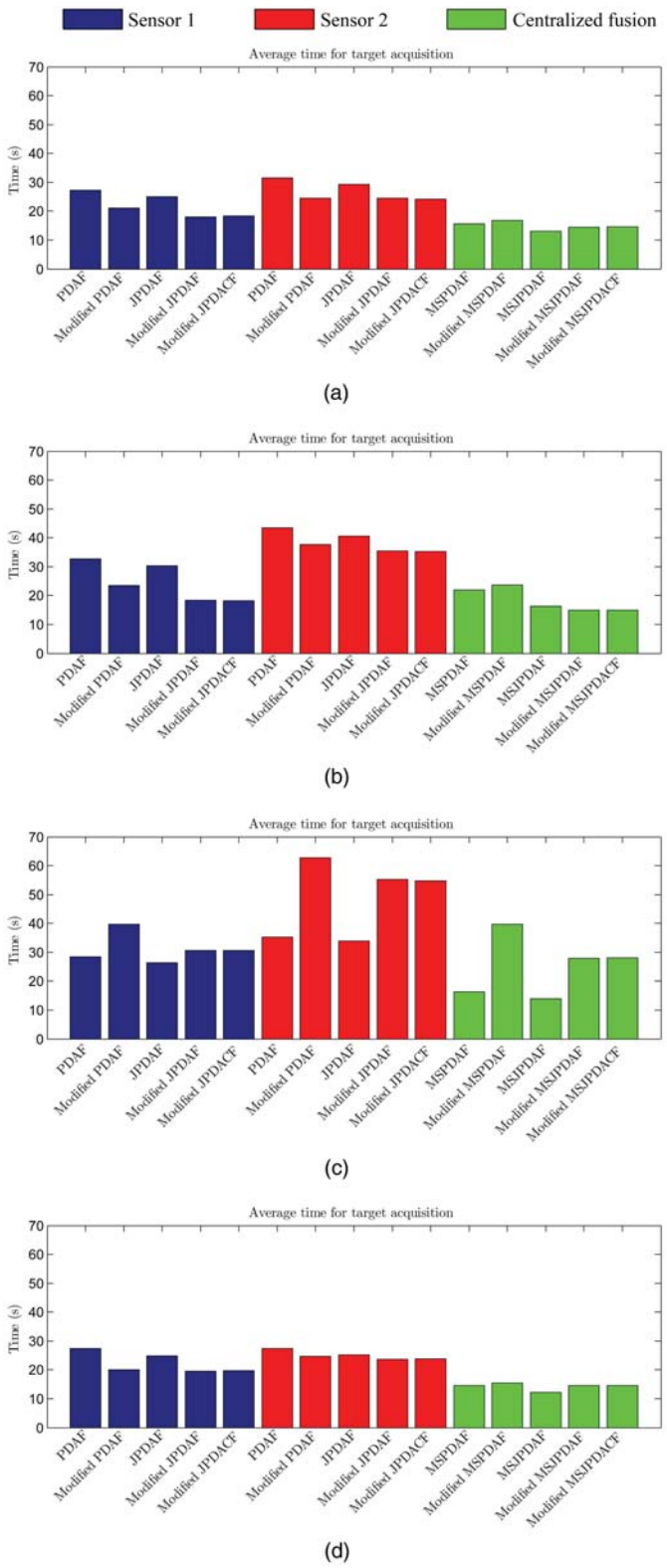

Fig. 11. Average time for target acquisition in the four simulation scenarios. (a) Scenario 1: Crossing trajectories. (b) Scenario 2: Parallel trajectories. (c) Scenario 3: Sequential trajectories. (d) Scenario 4: Meeting trajectories.

ing. As discussed above, the totally opposite velocities of the two targets and the high wake density in the whole joint validation region, make the targets' passing relatively easy.

In the sequential scenario the targets are never closer than about 5 m, so the RMS error does not increase much during the period the tracks are following after each other. In this scenario, the modified single target

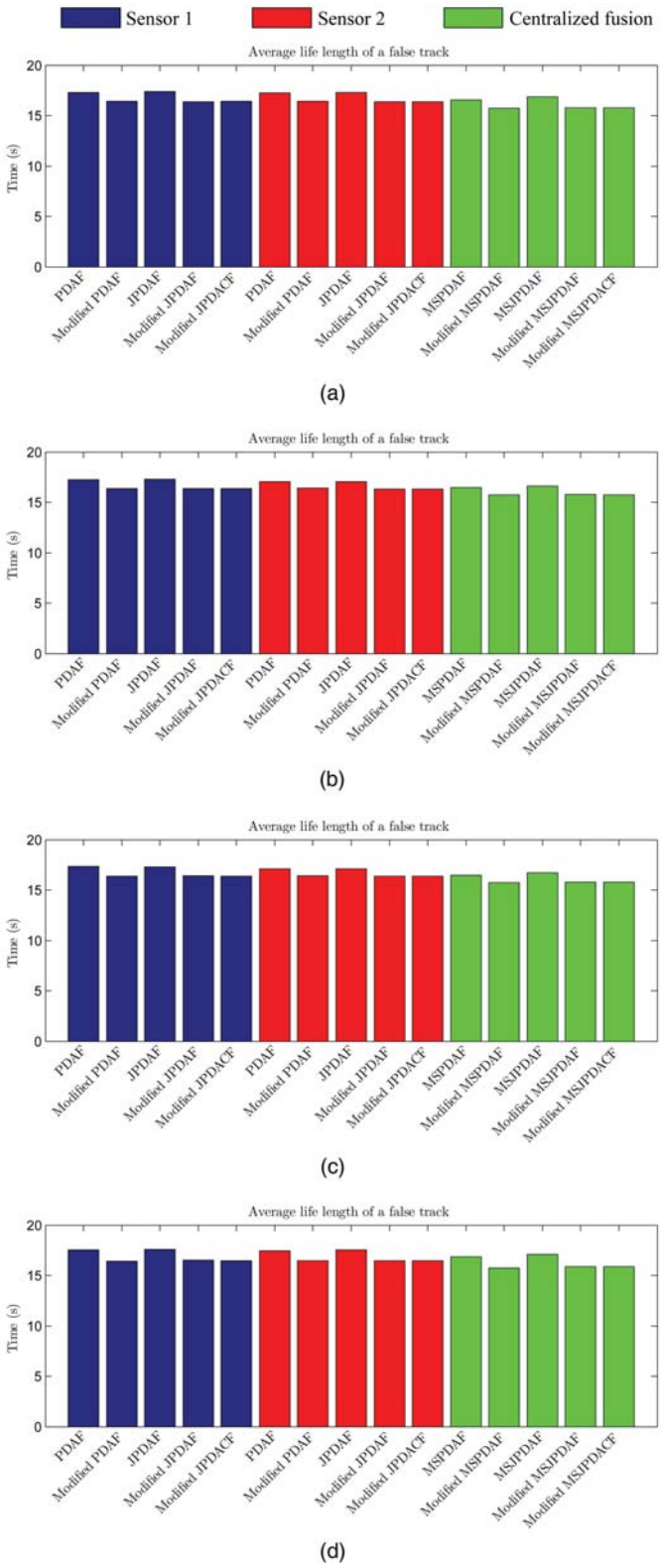

Fig. 12. Average track length for a false track in the four simulation scenarios. (a) Scenario 1: Crossing trajectories. (b) Scenario 2: Parallel trajectories. (c) Scenario 3: Sequential trajectories. (d) Scenario 4: Meeting trajectories.

tracking filter performs better than the modified multitarget tracking filters. The reason for this is because the RMS error is measured only among the true tracks, not when they become lost. In this scenario, where the targets are following after each other, the estimation error is larger for the target behind the one in front, because it is surrounded by wakes. From the percentage of lost tracks in Fig. 7, the modified single target filter will lose the target more often than the modified multitarget filters, and it is most likely that the lost target is the

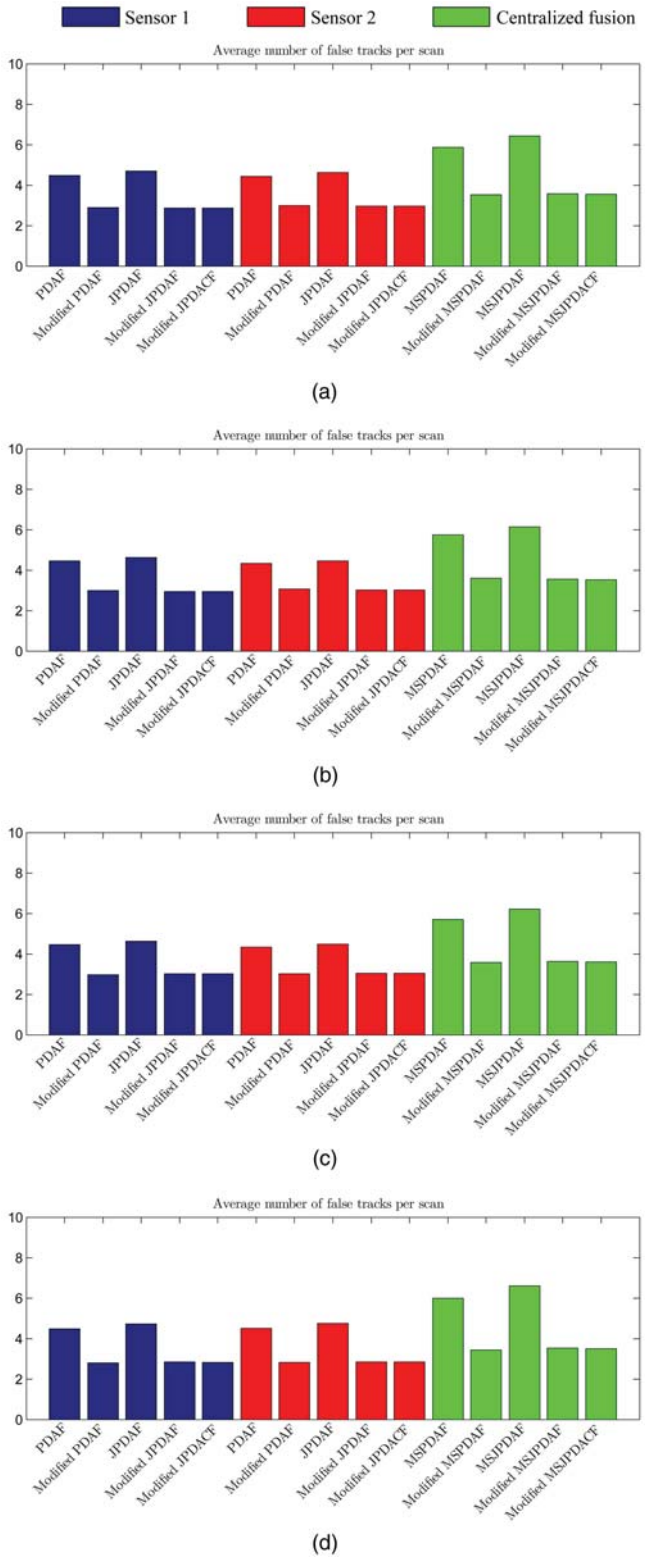

Fig. 13. Average number of false tracks per scan in the four simulation scenarios. (a) Scenario 1: Crossing trajectories. (b) Scenario 2: Parallel trajectories. (c) Scenario 3: Sequential trajectories. (d) Scenario 4: Meeting trajectories.

one with largest estimation error. Therefore, when the RMS error is calculated, the modified multitarget filters are based on tracks with larger estimation error than what the modified single target filter is based on, only because these tracks were not lost.

5.6 Usage of the Wake Model on Targets Without Wakes

In this section the erroneous use of wake models on targets without wakes is considered. The crossing sce-

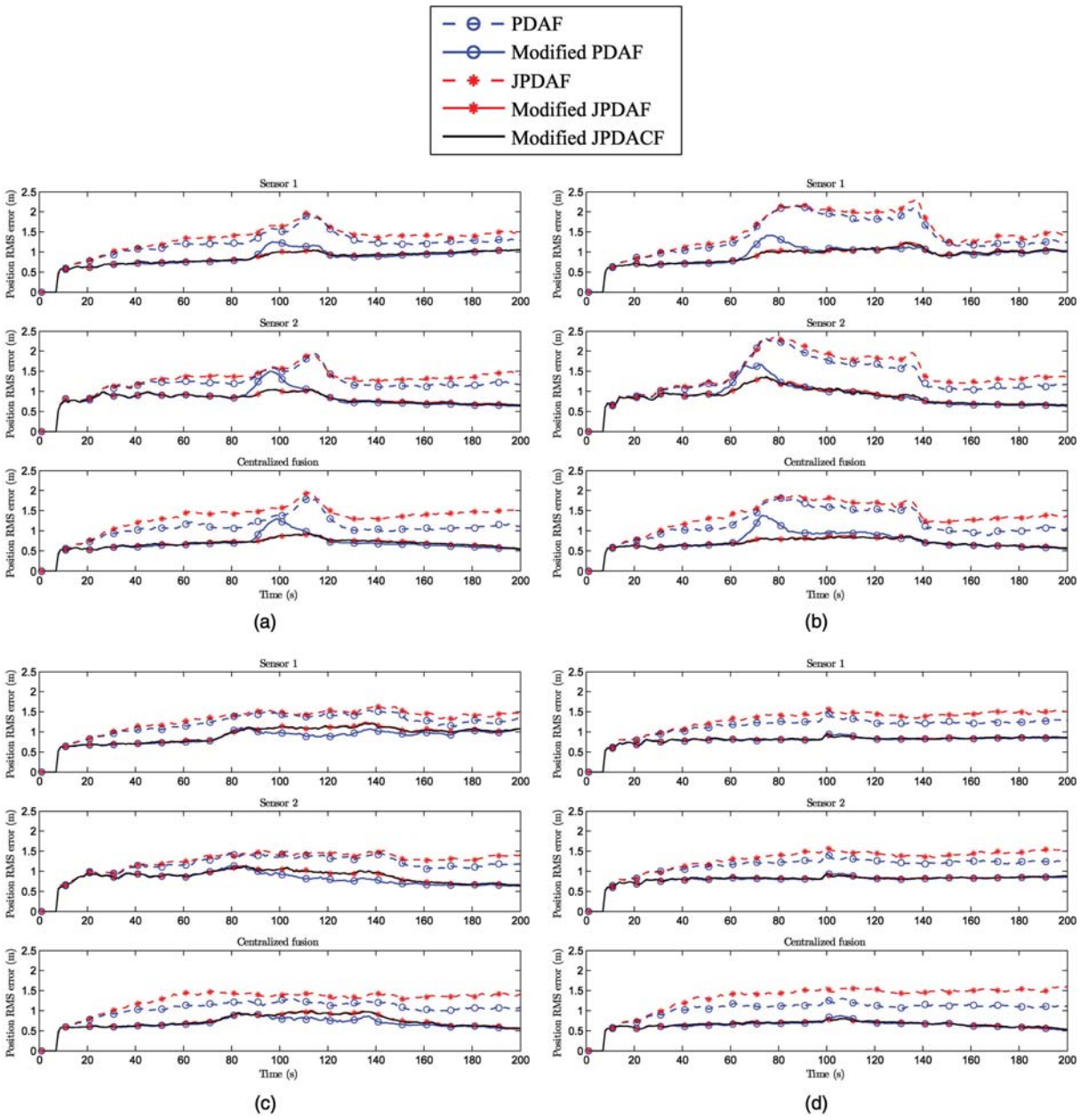

Fig. 14. Position RMS error from 500 Monte Carlo runs in: (a) Scenario 1: Crossing trajectories, (b) Scenario 2: Parallel trajectories, (c) Scenario 3: Sequential trajectories, (d) Scenario 4: Meeting trajectories.

nario (see Fig. 4) is used as before, but without wakes behind the targets.[2] Each target is simulated as a point-target (only one measurement) with detection probability $P_D = 0.7$, independently across time. The results after 500 Monte Carlo runs are shown in Fig. 15, and the performance is clearly better than in the wake-scenario due to the fact that each target is never simulated by more than one detection at a time. This shows that the scattering effect in real sensors, due to the beamforming, makes the tracking problem considerably harder and is an important element in further research.

It is also interesting to see that even though the modified PDAF performs worse than the standard PDAF, the modified multitarget algorithms perform almost the same as the standard JPDAF. This indicates that applying the modified JPDAF or JPDACF on targets without wakes will not degrade the tracking performance. For tracking in environments with different kinds of targets, with and without wakes, this is a desirable property.

Another issue worth mentioning is the increasing trend of the position RMS error for Sensor 1, and the decreasing trend for Sensor 2. This is due to the fact that the estimated position error increases with the distance to the sensors, and the targets are starting close to Sensor 1, and moving towards Sensor 2. Notice how

[2]This would correspond to "closed breathing system" scuba divers or mechanical underwater vehicles.

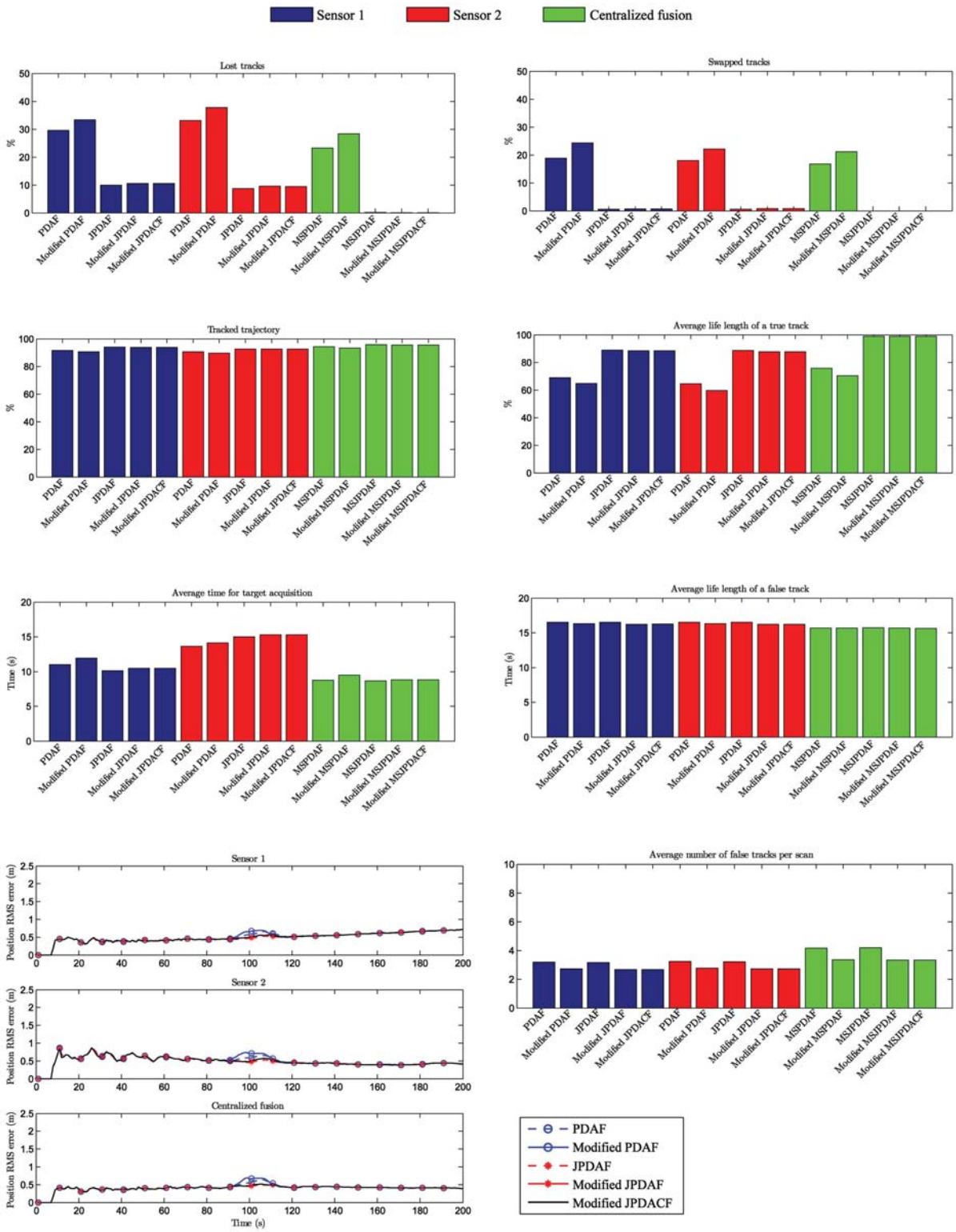

Fig. 15. Simulation results from the crossing scenario where the probabilistic wake model is erroneous applied to targets without wakes. Each target is simulated as point detections with detection probability $P_D = 0.7$, independent across time. The different features discussed in Section 5.5 are shown.

these trends in the single sensors are averaged out in the centralized tracking where the sensors' data are fused.

It is also shown that the use of multiple sensors is more effective in preventing lost tracks in this special case than in the previous cases where the targets had wakes. This gives an another justification of using multiple sensors when tracking targets in the presence of wakes, because a target could be mistaken for having a wake even when it does not have one.

6. CONCLUSIONS

An important factor in a multitarget tracking system is to correctly associate each measurement received from a detector to its origin. The JPDAF has been a solution to this problem due to its effectiveness and low computational demand. In the JPDAF all false measurements are assumed due to i.i.d. uniformly spatially distributed noise or clutter. This assumption is not adequate for targets that generate wakes, because detections originating from the wake are not uniformly distributed and may result in a lost track if they are not properly modelled. The solution presented incorporates a model of the wakes behind the targets in a multitarget environment. The purpose of this wake model is to weight wake-originated measurements lower than in a regular JPDAF to avoid the tracks following these measurements and therefore be forced to turn into the wake. To achieve this, we presented a model formed by the sum of single models each linearly increasing behind their associated targets.

A systematic comparison of the standard data association filters (PDAF and JPDAF) and their corresponding modified versions are presented in a multitarget multisensor environment. Four different simulation scenarios are examined where two targets in the presence of wakes are crossing, moving in parallel to each other, one following after another, and finally meeting and then passing each other. It is shown that the wake model presented is a useful modification of the JPDAF in all four scenarios. The only stated drawback using the wake model is when a target is moving after another one, surrounded by the wake from the target in front. In that case, if the rear target is lost, it is harder to reacquire the track because the measurements are assumed originating from the wake and not the true target.

This paper also presents the coupled version of the JPDAF, called JPDACF, and a modified JPDACF (with a wake model) is developed and tested. The simulations show that the modified JPDACF is not improving the performance compared to the simpler modified JPDAF, indicating that there is no significant correlation between the targets' estimation errors.

The simulation scenarios consider two sensors, and the data association filters at the local sensors are compared with multisensor (MS) filters in a centralized tracking configuration. A sequential state updating scheme is used in the multisensor filters, and the results show that the data fusion provides significant improvement in the tracking performance.

This paper also examines the effect of applying the wake model on point-targets without wakes. The results show that the modified JPDAF and JPDACF perform almost the same as the standard JPDAF. This makes the modification practical for real systems where both targets with wakes and targets without wakes are operating in the same environment.

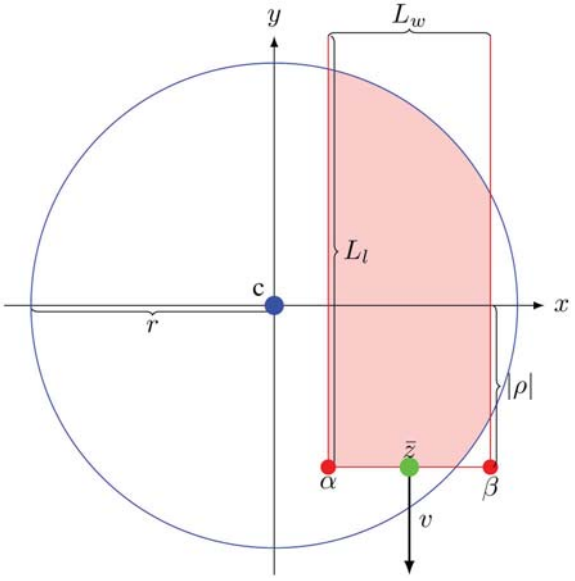

Fig. 16. Specification of variables for integration of the wake model, with length L_l and width L_w, inside the joint validation region with center c and radius r. The wake has front corners $[\alpha\ \rho]$ and $[\beta\ \rho]$ and is oriented behind the target with position $\bar{z}$ and velocity v.

APPENDIX A. SPECIFICATION OF THE JOINT WAKE MODEL

In this appendix the joint wake model $p_W(z_k)$ introduced in Section 3 is presented, and an analytical expression for the probability P_{GW} is derived. The joint wake model is the sum of all N_T single wake models $p_W^t(z_k)$ behind each target t under consideration

$$p_W(z_k) = \frac{1}{N_T}\sum_{t=1}^{N_T} p_W^t(z_k). \tag{54}$$

Next, consider the single wake model $p_W^t(z_k)$ of target t, and let $\bar{z}$ and v be the predicted position and velocity of the target, respectively. Reference to Fig. 16 may be helpful in the following. The single wake model is assumed linearly increasing with length L_l behind the predicted position of the target, i.e., in the direction opposite to v, and uniform with width L_w in the direction perpendicular to the target's velocity v. This model can be expressed by defining the independent variables l and w as the respective distances behind and sideways (relative to v) to the target. From the above assumption, l and w have the following densities

$$\begin{aligned} p_l(l) &= \frac{2l}{L_l^2} \qquad 0 \le l \le L_l \\ p_w(w) &= \frac{1}{L_w} \qquad 0 \le w \le \frac{L_w}{2} \end{aligned} \tag{55}$$

which yields

$$p_W^t(z_k) = p_l(l)p_w(w) = \frac{2l}{L_l^2 L_w}. \tag{56}$$

Notice that even though a current estimate of the velocity v is available in the filter, a better way in practice is to use an average of the latest estimates since the wake will not change direction as rapidly as the current target velocity estimate. In the simulations an average of the latest 6 estimates is used.

The joint validation region containing all candidate measurements in the multitarget environment is defined as a circle with radius r and center c. The center c is calculated as the average between all the predicted target positions, and the radius r is defined as the distance to the farthest validated measurement.

The probability P_{GW} in (25), used to restrict the density of the joint wake model $p_W(z_k)$ to the joint validation region, has to be calculated for each scan by integration of $p_W(z_k)$ inside the region. Since $p_W(z_k)$ is the sum of all single wake models $p_W^t(z_k)$, P_{GW} is obtained by calculating P_{GW}^t for each target t and then summing them up

$$P_{GW} = \sum_{t=1}^{N_T} P_{GW}^t. \tag{57}$$

The calculation of P_{GW}^t is derived next. Assume a Cartesian coordinate system with origin at position c and y-axis parallel to v but in the opposite direction, see Fig. 16. Define the two front corners of the wake model with elements α and β for the x-axis, and ρ for the y-axis

$$\begin{aligned} \rho &= (c-\bar{z})^T v/|v| \\ \alpha &= \sqrt{|c-\bar{z}|^2-\rho^2} - w/2 \\ \beta &= \sqrt{|c-\bar{z}|^2-\rho^2} + w/2. \end{aligned} \tag{58}$$

The integration depends on if the front corners $[\alpha \ \ \rho]^T$ and $[\beta \ \ \rho]^T$ are inside or outside the joint validation region (circle), and will be broken into one, two or three parts. To do this, define three binary variables δ_ρ, δ_α and δ_β as follows:

$$\delta_\rho = \begin{cases} 1 & \text{if} \quad \rho < 0 \\ 0 & \text{otherwise} \end{cases} \tag{59}$$

$$\delta_\alpha = \begin{cases} 1 & \text{if} \quad \sqrt{\alpha^2+\rho^2} > r \\ 0 & \text{otherwise} \end{cases} \tag{60}$$

$$\delta_\beta = \begin{cases} 1 & \text{if} \quad \sqrt{\beta^2+\rho^2} > r \\ 0 & \text{otherwise} \end{cases}. \tag{61}$$

Then the integral can be written as

$$\begin{aligned} P_{GW}^t = \frac{2}{L_l^2 L_w} \Bigg\{ & \delta_\rho \delta_\alpha \int_{\max(\alpha,-r)}^{-\sqrt{r^2-\rho^2}} \int_{-\sqrt{r^2-x^2}}^{\sqrt{r^2-x^2}} (y-\rho)dy\,dx \\ & + \int_{\alpha(1-\delta_\alpha)-\delta_\alpha\sqrt{r^2-\rho^2}}^{\beta(1-\delta_\beta)+\delta_\beta\sqrt{r^2-\rho^2}} \int_{\rho}^{\sqrt{r^2-x^2}} (y-\rho)dy\,dx \\ & + \delta_\rho \delta_\beta \int_{\sqrt{r^2-\rho^2}}^{\min(\beta,r)} \int_{-\sqrt{r^2-x^2}}^{\sqrt{r^2-x^2}} (y-\rho)dy\,dx \Bigg\}. \end{aligned} \tag{62}$$

For simplicity we substitute the limits of integration along the x-axis as follows:

$$\begin{aligned} a &= \max(\alpha, -r) \\ b &= -\sqrt{r^2-\rho^2} \\ c &= \alpha(1-\delta_\alpha) - \delta_\alpha\sqrt{r^2-\rho^2} \\ d &= \beta(1-\delta_\beta) + \delta_\beta\sqrt{r^2-\rho^2} \\ e &= \sqrt{r^2-\rho^2} \\ f &= \min(\beta, r) \end{aligned} \tag{63}$$

which yields

$$\begin{aligned} P_{GW}^t = & \frac{2}{L_l^2 L_w} \Bigg\{ \delta_\rho \delta_\alpha \int_a^b \int_{-\sqrt{r^2-x^2}}^{\sqrt{r^2-x^2}} (y-\rho)dy\,dx \\ & + \int_c^d \int_\rho^{\sqrt{r^2-x^2}} (y-\rho)dy\,dx \\ & + \delta_\rho \delta_\beta \int_e^f \int_{-\sqrt{r^2-x^2}}^{\sqrt{r^2-x^2}} (y-\rho)dy\,dx \Bigg\} \\ = & \frac{1}{L_l^2 L_w} \Bigg\{ \rho r^2 \left(\arcsin\frac{c}{r} - \arcsin\frac{d}{r} \right) \\ & + \frac{c^3-d^3}{3} + 2\rho\delta_\alpha\delta_\rho \left(a\sqrt{r^2-a^2} - b\sqrt{r^2-b^2} \right) \\ & - c(\rho^2+r^2) + 2\rho\delta_\beta\delta_\rho \left(e\sqrt{r^2-e^2} - f\sqrt{r^2-f^2} \right) \\ & + d(\rho^2+r^2) + 2\rho\delta_\alpha\delta_\rho r^2 \left(\arcsin\frac{a}{r} - \arcsin\frac{b}{r} \right) \\ & + \rho c\sqrt{r^2-c^2} + 2\rho\delta_\beta\delta_\rho r^2 \left(\arcsin\frac{e}{r} - \arcsin\frac{f}{r} \right) \\ & - \rho d\sqrt{r^2-d^2} \Bigg\}. \end{aligned} \tag{64}$$

APPENDIX B. COVARIANCE UPDATE IN THE MODIFIED JPDACF

In this section the updated stacked covariance for the JPDACF in (47) is derived. The updated covariance $P_{k|k}^S$, conditioned on all measurements up to time k, Z^k, is

$$P_{k|k}^S = E\{[x_k^S - \hat{x}_{k|k}^S][x_k^S - \hat{x}_{k|k}^S]^T \mid Z^k\}. \tag{65}$$

This can be expressed as a weighted sum of all joint association event conditioned estimation error covariances by using the total probability theorem

$$\begin{aligned} P_{k|k}^S = & \sum_{\Theta_k} P\{\Theta_k \mid Z^k\} \\ & \times E\{[x_k^S - \hat{x}_{k|k}^S][x_k^S - \hat{x}_{k|k}^S]^T \mid Z^k, \Theta_k\}. \end{aligned} \tag{66}$$

Let $\hat{x}_{k|k}^S(\Theta)$ be the state estimate conditioned on the joint association event Θ_k. By using this, (66) can be

rewritten as

$$
\begin{aligned}
P^S_{k|k} &= \sum_{\Theta_k} P\{\Theta_k \mid Z^k\} \\
&\quad \times E\left\{[(x^S_k - \hat{x}^S_{k|k}(\Theta) + \hat{x}^S_{k|k}(\Theta) - \hat{x}^S_{k|k})] \right. \\
&\qquad \left. \times [(x^S_k - \hat{x}^S_{k|k}(\Theta) + \hat{x}^S_{k|k}(\Theta) - \hat{x}^S_{k|k})]^T \mid Z^k, \Theta_k \right\} \\
&= \sum_{\Theta_k} P\{\Theta_k \mid Z^k\} \\
&\quad \times E\left\{(x^S_k - \hat{x}^S_{k|k}(\Theta))(x^S_k - \hat{x}^S_{k|k}(\Theta))^T \right. \\
&\qquad + (x^S_k - \hat{x}^S_{k|k}(\Theta))(\hat{x}^S_{k|k}(\Theta) - \hat{x}^S_{k|k})^T \\
&\qquad + (\hat{x}^S_{k|k}(\Theta) - \hat{x}^S_{k|k})(x^S_k - \hat{x}^S_{k|k}(\Theta))^T \\
&\qquad \left. + (\hat{x}^S_{k|k}(\Theta) - \hat{x}^S_{k|k})(\hat{x}^S_{k|k}(\Theta) - \hat{x}^S_{k|k})^T \mid Z^k, \Theta_k \right\} \\
&= \sum_{\Theta_k} P\{\Theta_k \mid Z^k\} \\
&\quad \times E\{(x^S_k - \hat{x}^S_{k|k}(\Theta))(x^S_k - \hat{x}^S_{k|k}(\Theta))^T \mid Z^k, \Theta_k\} \\
&\quad + \sum_{\Theta_k} P\{\Theta_k \mid Z^k\} \\
&\quad \times (\hat{x}^S_{k|k}(\Theta) - \hat{x}^S_{k|k})(\hat{x}^S_{k|k}(\Theta) - \hat{x}^S_{k|k})^T \\
&= \sum_{\Theta_k} P\{\Theta_k \mid Z^k\} \\
&\quad \underbrace{\times E\{(x^S_k - \hat{x}^S_{k|k}(\Theta))(x^S_k - \hat{x}^S_{k|k}(\Theta_k))^T \mid Z^k, \Theta_k\}}_{P_\Theta} \\
&\quad \underbrace{+ \sum_{\Theta_k} P\{\Theta_k \mid Z^k\} \hat{x}^S_{k|k}(\Theta)\hat{x}^S_{k|k}(\Theta)^T - \hat{x}^S_{k|k}(\hat{x}^S_{k|k})^T}_{\tilde{P}} \\
&= \sum_{\Theta_k} P\{\Theta_k \mid Z^k\} P_\Theta + \tilde{P}
\end{aligned} \tag{67}
$$

where the identity

$$
\sum_{\Theta_k} P\{\Theta_k \mid Z^k\} = 1 \tag{68}
$$

is used together with the fact that

$$
\hat{x}^S_{k|k}(\Theta) = E\{x^S_k \mid Z^k, \Theta_k\} \tag{69}
$$

$$
\hat{x}^S_{k|k} = \sum_{\Theta_k} P\{\Theta_k \mid Z^k\} \hat{x}^S_{k|k}(\Theta). \tag{70}
$$

Next, P_Θ in the first term of (67) will be derived

$$
P_\Theta = E\{(x^S_k - \hat{x}^S_{k|k}(\Theta))(x^S_k - \hat{x}^S_{k|k}(\Theta))^T \mid Z^k, \Theta\} \tag{71}
$$

where the conditioned estimation error is

$$
\begin{aligned}
\tilde{x}^S_k(\Theta) &= x^S_k - \hat{x}^S_{k|k}(\Theta) \\
&= F^S x^S_{k-1} + v^S_{k-1} - F^S \hat{x}^S_{k-1|k-1} - I^x_\Theta W^S_k I^z_\Theta \nu^S_k(\Theta).
\end{aligned} \tag{72}
$$

Substituting (under the assumption that all targets are observed)

$$
\begin{aligned}
\nu^S_k(\Theta) &= z^S_k(\Theta) - H^S F^S \hat{x}^S_{k-1|k-1} \\
&= H^S F^S x^S_{k-1} + H^S v^S_{k-1} + w^S_k - H^S F^S \hat{x}^S_{k-1|k-1} \\
&= H^S F^S \tilde{x}^S_{k-1} + H^S v^S_{k-1} + w^S_k
\end{aligned} \tag{73}
$$

in (72) yields

$$
\begin{aligned}
\tilde{x}^S_k(\Theta) &= (I - I^x_\Theta W^S_k I^z_\Theta H^S) F^S \tilde{x}^S_{k-1} \\
&\quad + (I - I^x_\Theta W^S_k I^z_\Theta H^S) v^S_{k-1} - I^x_\Theta W^S_k I^z_\Theta w^S_k.
\end{aligned} \tag{74}
$$

Using this in (71) gives

$$
\begin{aligned}
P_\Theta &= (I - I^x_\Theta W^S_k I^z_\Theta H^S) P^S_{k|k-1} (I - I^x_\Theta W^S_k I^z_\Theta H^S)^T \\
&\quad + I^x_\Theta W^S_k I^z_\Theta R^S I^z_\Theta W^{S^T}_k I^x_\Theta
\end{aligned} \tag{75}
$$

where

$$
P^S_{k|k-1} = F^S P^S_{k-1|k-1} F^{S^T} + Q^S. \tag{76}
$$

In (75) the assumptions in (2) are used together with the following independence assumptions between the estimation error and the two noises

$$
E\{\tilde{x}^S_k v^{S^T}_k \mid Z^k, \Theta_k\} = 0 \tag{77}
$$

$$
E\{\tilde{x}^S_{k-1} w^{S^T}_k \mid Z^k, \Theta_k\} = 0. \tag{78}
$$

The last term $\tilde{P}$ in (67) is

$$
\begin{aligned}
\tilde{P} &= \sum_{\Theta_k} P\{\Theta_k \mid Z^k\} \hat{x}^S_{k|k}(\Theta)\hat{x}^S_{k|k}(\Theta)^T - \hat{x}^S_{k|k}(\hat{x}^S_{k|k})^T \\
&= \sum_{\Theta_k} P\{\Theta_k \mid Z^k\} (\hat{x}^S_{k|k-1} + I^x_\Theta W^S_k I^z_\Theta \nu^S_k(\Theta)) \\
&\quad \times (\hat{x}^S_{k|k-1} + I^x_\Theta W^S_k I^z_\Theta \nu^S_k(\Theta))^T \\
&\quad - \left(\hat{x}^S_{k|k-1} + \sum_{\Theta_k} P\{\Theta_k \mid Z^k\} I^x_\Theta W^S_k I^z_\Theta \nu^S_k(\Theta) \right) \\
&\quad \times \left(\hat{x}^S_{k|k-1} + \sum_{\Theta_k} P\{\Theta_k \mid Z^k\} I^x_\Theta W^S_k I^z_\Theta \nu^S_k(\Theta) \right)^T
\end{aligned} \tag{79}
$$

which after cancellations becomes the spread of innovations

$$
\begin{aligned}
\tilde{P} &= \sum_{\Theta_k} P\{\Theta_k \mid Z^k\} I^x_\Theta W^S_k I^z_\Theta \nu^S_k(\Theta) \nu^S_k(\Theta)^T I^z_\Theta W^{S^T}_k I^x_\Theta \\
&\quad - \left(\sum_{\Theta_k} P\{\Theta_k \mid Z^k\} I^x_\Theta W^S_k I^z_\Theta \nu^S_k(\Theta) \right) \\
&\quad \times \left(\sum_{\Theta_k} P\{\Theta_k \mid Z^k\} I^x_\Theta W^S_k I^z_\Theta \nu^S_k(\Theta) \right)^T.
\end{aligned} \tag{80}
$$

Using (80) and (75) in (67) yields the updated stacked covariance

$$
\begin{aligned}
P^S_{k|k} = &\sum_{\Theta_k} P\{\Theta_k \mid Z^k\} \\
&\times \Big\{ I^x_\Theta W^S_k I^z_\Theta (\nu^S_k(\Theta)\nu^S_k(\Theta)^T + R^S) I^z_\Theta W^{S\,T}_k I^x_\Theta \\
&\quad + (I - I^x_\Theta W^S_k I^z_\Theta H^S) P^S_{k|k-1} (I - I^x_\Theta W^S_k I^z_\Theta H^S)^T \Big\} \\
&- \left(\sum_{\Theta_k} P\{\Theta_k \mid Z^k\} I^x_\Theta W^S_k I^z_\Theta \nu^S_k(\Theta) \right) \\
&\times \left(\sum_{\Theta_k} P\{\Theta_k \mid Z^k\} I^x_\Theta W^S_k I^z_\Theta \nu^S_k(\Theta) \right)^T . \qquad (81)
\end{aligned}
$$

REFERENCES

[1] M. Athans, R. H. Whiting and M. Gruber
A suboptimal estimation algorithm with probabilistic editing for false measurements with applications to target tracking with wake phenomena.
IEEE Transactions on Automatic Control, **22**, 3 (June 1977), 372–384.

[2] Y. Bar-Shalom, K. C. Chang and H. A. P. Blom
Tracking of splitting targets in clutter using an interacting multiple model joint probabilistic data association filter.
In *Proceedings of the 30th IEEE Conference on Decision and Control*, Brighton, UK, Dec. 1991, 2043–2048.

[3] Y. Bar-Shalom and X. R. Li
Multitarget-Multisensor Tracking: Principles and Techniques.
Storrs, CT: YBS Publishing, 1995.

[4] Y. Bar-Shalom, X. R. Li and T. Kirubarajan
Estimation with Application to Tracking and Navigation.
New York: Wiley-Interscience, 2001.

[5] Y. Bar-Shalom
Tracking methods in a multitarget environment.
IEEE Transactions on Automatic Control, **23**, 4 (1978), 618–626.

[6] D. K. Barton
Modern Radar System Analysis.
Norwood, MA: Artech House, 1988.

[7] S. Blake and S. Watts
A multitarget track-while-scan filter.
In *Proceedings of the IEE Radar 87 Conference*, London, England, Oct. 1987.

[8] E. A. Bloem and H. A. P. Blom
Joint probabilistic data association methods avoiding track coalescence.
In *Proceedings of the 34th IEEE Conference on Decision and Control*, vol. 3, New Orleans, LA, Dec. 1995, 2752–2757.

[9] H. A. P. Blom and E. A. Bloem
Probabilistic data association avoiding track coalescence.
IEEE Transactions on Automatic Control, **45**, 2 (Feb. 2000), 247–259.

[10] H. Chen, T. Kirubarajan and Y. Bar-Shalom
Comparison of centralized and distributed tracking algorithms using air-to-air scenarios.
In *Proceedings of the SPIE Conference on Signal and Data Processing of Small Targets*, vol. 4048, July 2000, 440–451.

[11] H. Chen, T. Kirubarajan and Y. Bar-Shalom
Performance limits of track-to-track fusion versus centralized estimation: Theory and application [sensor fusion].
IEEE Transactions on Aerospace and Electronic Systems, **39**, 2 (Apr. 2003), 386–400.

[12] H. Chen, K. Zhang and X. R. Li
Optimal data compression for multisensor target tracking with communication constraints.
In *Proceedings of the 43rd IEEE Conference on Decision and Control*, vol. 3, Dec. 2004, 2650–2655.

[13] R. J. Fitzgerald
Development of practical PDA logic for multitarget tracking by microprocessor.
In Y. Bar-Shalom (Ed.), *Multitarget Multisensor Tracking*, Norwood, MA: Artech House, 1990, 1–23.

[14] T. E. Fortmann, Y. Bar-Shalom and M. Scheffe
Sonar tracking of multiple targets using joint probabilistic data association.
IEEE Journal of Oceanic Engineering, **8**, 3 (July 1983), 173–184.

[15] P. P. Gandhi and S. A. Kassam
Analysis of CFAR processors in homogeneous background.
IEEE Transactions on Aerospace and Electronic Systems, **24**, 4 (July 1988), 427–445.

[16] X. Lurton
An Introduction to Underwater Acoustics.
New York: Springer, 2002.

[17] D. Musicki and R. Evans
Joint integrated probabilistic data association: JIPDA.
IEEE Transactions on Aerospace and Electronic Systems, **40**, 3 (July 2004), 1093–1099.

[18] D. Musicki, R. Evans and S. Stankovic
Integrated probabilistic data association.
IEEE Transactions on Automatic Control, **39**, 6 (June 1994), 1237–1241.

[19] L. Y. Pao and C. W. Frei
A comparison of parallel and sequential implementations of a multisensor multitarget tracking algorithm.
In *Proceedings of the American Control Conference*, vol. 3, Seattle, WA, June 1995, 1683–1687.

[20] A. Papoulis and S. U. Pillai
Probability, Random Variables and Stochastic Processes 4th Edition.
New York: McGraw-Hill, 2002.

[21] A. Rødningsby and Y. Bar-Shalom
Tracking of divers using a probabilistic data association filter with a bubble model.
IEEE Transactions on Aerospace and Electronic Systems, 2009.

[22] A. Rødningsby, Y. Bar-Shalom, O. Hallingstad and J. Glattetre
Multitarget tracking in the presence of wakes.
In *Proceedings of the 11th International Conference on Information Fusion*, Cologne, Germany, 2008, 1536–1543.

[23] J. P. Serra
Image Analysis and Mathematical Morphology.
London, UK: Academic Press, 1982.

[24] W. Smith
Modern Optical Engineering: The Design of Optical Systems (2nd ed.).
New York: McGraw-Hill, 1990.

[25] S. M. Tonissen and Y. Bar-Shalom
Maximum likelihood track-before-detect with fluctuating target amplitude.
IEEE Transactions on Aerospace and Electronic Systems, **34**, 3 (July 1998), 796–808.

[26] R. Urick
Principles of Underwater Sound (3rd ed.).
New York: McGraw-Hill, 1983.

Anders Rødningsby was born on May 19, 1979 in Kongsberg, Norway. He received the B.E. degree from Gjøvik University College, Norway, in electrical engineering and the M.S. degree from the University of Oslo, Norway, in applied mathematics, mechanics and numerical physics, in 2003 and 2005, respectively.

He is currently a research scientist at the Norwegian Defence Research Establishment (FFI), and a Ph.D. candidate at the Norwegian University of Science and Technology. His research interests include detection theory, navigation and target tracking.

Yaakov Bar-Shalom was born on May 11, 1941. He received the B.S. and M.S. degrees from the Technion, Israel Institute of Technology, in 1963 and 1967 and the Ph.D. degree from Princeton University in 1970, all in electrical engineering.

From 1970 to 1976 he was with Systems Control, Inc., Palo Alto, CA. Currently he is Board of Trustees Distinguished Professor in the Dept. of Electrical and Computer Engineering and Marianne E. Klewin Professor in Engineering at the University of Connecticut. He is also Director of the ESP (Estimation and Signal Processing) Lab.

His current research interests are in estimation theory and target tracking and has published over 370 papers and book chapters in these areas and in stochastic adaptive control. He coauthored the monograph *Tracking and Data Association* (Academic Press, 1988), the graduate texts *Estimation and Tracking: Principles, Techniques and Software* (Artech House, 1993), *Estimation with Applications to Tracking and Navigation: Algorithms and Software for Information Extraction* (Wiley, 2001), the advanced graduate text *Multitarget-Multisensor Tracking: Principles and Techniques* (YBS Publishing, 1995), and edited the books *Multitarget-Multisensor Tracking: Applications and Advances* (Artech House, Vol. I, 1990; Vol. II, 1992; Vol. III, 2000).

He has been elected Fellow of IEEE for "contributions to the theory of stochastic systems and of multitarget tracking." He has been consulting to numerous companies and government agencies, and originated the series of Multitarget-Multisensor Tracking short courses offered via UCLA Extension, at Government Laboratories, private companies and overseas.

During 1976 and 1977 he served as Associate Editor of the IEEE Transactions on Automatic Control and from 1978 to 1981 as Associate Editor of Automatica. He was Program Chairman of the 1982 American Control Conference, General Chairman of the 1985 ACC, and Co-Chairman of the 1989 IEEE International Conference on Control and Applications. During 1983–87 he served as Chairman of the Conference Activities Board of the IEEE Control Systems Society and during 1987–89 was a member of the Board of Governors of the IEEE CSS. He was a member of the Board of Directors of the International Society of Information Fusion (1999–2004) and served as General Chairman of FUSION 2000, President of ISIF in 2000 and 2002 and Vice President for Publications in 2004–08.

In 1987 he received the IEEE CSS Distinguished Member Award. Since 1995 he is a Distinguished Lecturer of the IEEE AESS and has given numerous keynote addresses at major national and international conferences. He is corecipient of the M. Barry Carlton Award for the best paper in the IEEE Transactions on Aerospace and Electronic Systems in 1995 and 2000 and the 1998 University of Connecticut AAUP Excellence Award for Research. In 2002 he received the J. Mignona Data Fusion Award from the DoD JDL Data Fusion Group. He is a member of the Connecticut Academy of Science and Engineering. He is the recipient of the 2008 IEEE Dennis J. Picard Medal for Radar Technologies and Applications.

Oddvar Hallingstad was born on October 17, 1945 in Hol, Norway. He received the M.E. degree from the Norwegian Technical University (NTH) in 1971 and his Ph.D. in 1978 also from NTH. His thesis covered "Transient stability models: Parameter estimation and model reduction."

Oddvar joined the Norwegian Defence Research Establishment (FFI) in 1977 where he worked on the inertial navigation system for the new costal vessels and the inertial navigation system for the Penguin air to sea missile. Since 1989 he has been at The Graduate University Center at Kjeller lecturing estimation theory and being an advisor for master and Ph.D. students. He is also an adjunct professor at The Norwegian University of Science and Technology (NTNU) and a part-time employee at FFI.

John Glattetre was born on November 7, 1944 in Brooklyn, NY and moved to Norway in 1957. He received the B.E. from Oslo Technical College in 1971, the M.E. degree from the Norwegian Technical University in 1977 and his Ph.D. from the Norwegian Technical University in 1986. His thesis covered "Interaction between water borne waves and seismic waves in the ocean bottom: The forward- and inverse problem."

John was an authorized aircraft radio mechanic in SAS. He performed flight calibration of aeronautical navigation systems (VOR, ILS, VDF) for the Norwegian Directorate of Civil Aviation. After a short period with micro electronics, he joined the Norwegian Defence Research Establishment (FFI) as a research scientist and worked with sound propagation and signal processing in underwater acoustics. John presently does R & D for Kongsberg Maritime AS where his emphasis is on active sonar, sound propagation, design and signal processing including tracking. He is co-advisor for two Ph.D. students. John is a member of the Acoustical Society of America's Technical Committee on Underwater Acoustics.